

Pan-Arctic Ocean primary production constrained by turbulent nitrate fluxes

Achim Randelhoff^{12*}, Johnna Holding³⁴, Markus Janout⁵, Mikael Kristian Sejr³⁴, Marcel Babin¹², Jean-Éric Tremblay¹², Matthew B. Alkire⁶⁷

¹ Takuvik Joint International Laboratory, Université Laval (QC, Canada) and CNRS (France)

² Département de biologie and Québec-Océan, Université Laval (QC, Canada)

³ Arctic Research Centre, Aarhus University, Ny Munkegade 114, bldg. 1540, 8000 Aarhus C, Denmark

⁴ Department of Bioscience, Aarhus University, Vejlsøvej 25, 8600, Silkeborg, Denmark

⁵ Alfred-Wegener-Institute Helmholtz Center for Polar and Marine Research, Am Handelshafen 12, D-27570 Bremerhaven, Germany

⁶ Applied Physics Laboratory, University of Washington, Seattle, WA USA

⁷ Now at: School of Oceanography, University of Washington, Seattle, WA USA

* **Correspondance:**

Achim Randelhoff, achim.randelhoff@takuvik.ulaval.ca

Keywords: Arctic, turbulence, nitrate, flux, primary production, climate change, sea ice

Abstract

Arctic Ocean primary productivity is limited by light and inorganic nutrients. With sea ice cover declining in recent decades, nitrate limitation has been speculated to become more prominent. Although much has been learned about nitrate supply from general patterns of ocean circulation and water column stability, a quantitative analysis requires dedicated turbulence measurements that have only started to accumulate in the last dozen years. Here we present new observations of the turbulent vertical nitrate flux in the Laptev Sea, Baffin Bay, and Young Sound (North-East Greenland), supplementing a compilation of 13 published estimates throughout the Arctic Ocean. Combining all flux estimates with a Pan-Arctic database of in situ measurements of nitrate concentration and density, we found the annual nitrate inventory to be largely determined by the strength of stratification and by bathymetry. Nitrate fluxes explained the observed regional patterns and magnitudes of both new primary production and particle export on annual scales. We argue that with few regional exceptions, vertical turbulent nitrate fluxes can be a reliable proxy of Arctic primary production accessible through autonomous and large-scale measurements. They may also provide a framework to assess nutrient limitation scenarios based on clear energetic and mass budget constraints resulting from turbulent mixing and freshwater flows.

1 Introduction

Without upward mixing of nutrients, much of the ocean would harbour no life (Ambühl, 1959; Margalef, 1978); the Arctic Ocean is no exception. As dead algae and other particulate matter have the tendency to sink due to their higher density, nutrients are constantly removed from surface waters. Phytoplankton therefore relies on a resupply of nutrients to grow and re-build its standing stock every year. Consequently, primary production, occurring in the euphotic zone where light levels are sufficient to support net growth, is controlled by the vertical flux of new nutrients from below the photic zone each year and thus available to new production, i.e. uptake of allochthonous nitrate (see Appendix and Dugdale and Goering, 1967).

While turbulence is an important factor for aquatic life everywhere, the Arctic Ocean is special in certain regards such as a ubiquitous sea ice cover and strong stratification (Aagaard and Carmack, 1989). Large summertime accumulation of meltwater from sea ice and terrestrial runoff has profound impacts on vertical mixing in the upper ocean (Cole et al., 2018; McPhee and Kantha, 1989; Randelhoff et al., 2017). In winter, brine rejection from freezing ice weakens stratification and creates turbulence (McPhee and Stanton, 1996). We will show throughout this paper that winter mixing is disproportionately important for setting mixed-layer properties.

Sea ice is often assumed to be a rather rigid lid (Padman, 1995) that shuts out a large portion of the sunlight as well as wind energy that could otherwise mix the ocean. With continued decline of sea ice extent and thickness in the 21st century (Comiso, 2012; Meier et al., 2014; Stroeve et al., 2012), the factors limiting Arctic marine growth will likely change. Such a transition in limiting factors usually leads to difficulties in predicting systems (Allen and Hoekstra, 2015). Indeed, Vancoppenolle et al. (2013) found that three different coupled biogeochemical general circulation models and their predictions for integrated Arctic Ocean primary production until the end of this century show diverging trajectories with opposite trends beyond a few decades from now. In their analysis, a prominent uncertainty concerned the evolution of the nitrogen pool in the photic zone. Yet since phytoplankton growth is a rate and not a stock, one should ideally measure the nitrogen flux, not its concentration at a given time, to determine primary production in the long term. Our lack of understanding of the vertical nitrate flux has resulted in the failure to consistently predict future Arctic Ocean primary production.

Stratification inhibits vertical mixing (Osborn, 1980) and consequently vertical turbulent nitrate fluxes. The Arctic Ocean can be divided into a weakly stratified Atlantic sector and a strongly stratified Pacific one (e.g. Carmack, 2007; Bluhm et al., 2015; Tremblay et al., 2015). Vertical turbulent nitrate fluxes are therefore routinely invoked to explain patterns of primary production across the Arctic, such as basin scale differences (Carmack et al., 2006; Randelhoff and Guthrie, 2016; Tremblay et al., 2015), but also an apparently increasing prevalence of fall blooms (Ardyna et al., 2014; Nishino et al., 2015) and even fjord scale differences depending on glacier morphology (Hopwood et al., 2018). These observations are mostly qualitative and rarely quantified with direct measurements. Whereas the vertical nitrate flux in the world ocean has received attention at least since the late 1980s (Lewis et al., 1986), dedicated measurements in the Arctic Ocean have only started to accumulate in the last dozen years. We use this opportunity to summarize the current state of knowledge and investigate the role of vertical turbulent nitrate fluxes in regulating Arctic marine productivity. Interestingly, we find that vertical mixing largely explains marine primary productivity at the pan-Arctic scale. Finally, we outline further research directions to unify physical constraints of Arctic Ocean primary production.

2 Material & methods

This study compiles measurements and estimates of the upward vertical turbulent flux of nitrate in different locations across the Arctic Ocean. We present four new estimates of the turbulent vertical nitrate flux, along with a dozen more values derived from the literature. We further supplement the nitrate fluxes with a collection of vertical profiles of seawater nitrate concentration.

2.1 Compilation of NO_3^- concentrations

The Pan-Arctic data base carefully compiled by Codispoti et al. (2013) was downloaded from the NOAA website under NODC accession number 0072133. An additional database covered the Canadian Archipelago using various ArcticNet and Department of Fisheries and Oceans Canada cruises, compiled by Coupel et al. (2020, in prep.). We included more winter data, notoriously scarce in the Arctic, by downloading data from the Chukchi shelf as presented by Arrigo et al. (2017). For each profile, we derived (1) the Brunt-Väisälä buoyancy frequency in the depth interval from 30 to 60 m as an indicator of the strength of stratification and (2) the surface nitrate concentration. For the latter, only profiles were used where the depth of the shallowest nitrate measurement was at most 15 m. The shallowest nitrate measurement was then extrapolated to the surface (0 m depth), after which values were averaged over the interval 0-15 m.

2.2 Compilation of turbulent vertical nitrate fluxes

In order to compile previously published estimates of vertical turbulent nitrate fluxes in the Arctic Ocean, we relied mostly on our knowledge of the literature, given the small amount of relevant publications. Additionally, we performed a search on Web of Science (Clarivate Analytics) using the search term $\text{TS}=(\text{nitr}^* \text{ AND suppl}^*) \text{ OR } (\text{nitr}^* \text{ AND flux}^*) \text{ OR } (\text{nitr}^* \text{ AND mix}^*) \text{ AND TS}=(\text{Arctic OR Polar}) \text{ AND Ocean}) \text{ AND TS}=(\text{vertical OR turbulen}^*) \text{ AND WC}=\text{Ocean}^*$, which resulted in 95 publications that were individually screened for relevance. We only included measurements and estimates based on in-situ observations.

The resulting list comprised just above a dozen flux estimates going back to less than ten publications. To improve data coverage, we present new vertical nitrate flux estimates from the Laptev Sea, Baffin Bay, and Young Sound, as well as a re-calculation of published observations from the Chukchi Sea (Nishino et al., 2015). In order to not disrupt the flow of the main text, details of the respective methods and field campaigns are deferred to the Appendix.

Briefly, our three-week-long summer sampling campaign in Young Sound (a North East Greenland fjord) sought to quantify turbulent mixing, vertical nitrate supply, and new (nitrate-based) production in a fjord strongly stratified by meltwater from the Greenland Ice Sheet. From the Laptev Sea, we present a small selection of representative vertical profiles of nitrate concentrations and oceanic microstructure, collected in the years 2008-2018. From Baffin Bay, we made use of a novel year-long 2017-18 time series of autonomous profilers, so-called biogeochemical (BGC) Argo floats (Biogeochemical-Argo Planning Group, 2016). These were specially adapted in order to function under the ice cover lasting from November to July. Based on the evolution of the upper-ocean nitrate inventory, we inferred the part due to vertical mixing. We further used a data set of nitrate concentrations and turbulent microstructure in the Chukchi Sea (Nishino et al., 2015) to calculate another estimate of vertical nitrate fluxes during early fall.

For the majority of those experiments, turbulence (microstructure) data were measured; just as was the case for the literature values. In some cases, turbulent mixing was inferred from current finestructure; see also the Appendix. Nitrate fluxes were calculated across the nitracline, meaning by combining a nitracline-average turbulent diffusivity with the strength of the nitrate gradient. Individual methodologies may however vary regarding e.g. choice of vertical layer or averaging procedures. According to our personal experience, such choices may make a difference for individual calculations, but less so for large-scale averages, and therefore we take the fluxes recorded in the literature at face value. A systematic assessment of potential methodological errors has to our knowledge however not been conducted. For a more detailed discussion of how vertical nitrate fluxes are measured, and in particular the uncertainties and caveats that come with each method, see the Appendix.

For each of the estimates of the vertical turbulent nitrate flux across the nitracline and into the surface layer, we extracted the end-of-winter surface nitrate concentration either from the same publication or from related studies. We also classified each nitrate flux value as either “perennial stratification” or “winter overturning”. The former means that surface layer stratification persisted year-round; the latter means that the winter mixed layer was significantly deeper than the meltwater-stratified summer surface layer. The classification was done based on perusal of the available literature. The full rationale with a detailed description of the vertical layering in relation to the nitrogen budget is given in the Appendix.

The specific references for each data point are given in the supplementary material. Our entire data set is presented in Table 1; note that it mixes vertical nitrate fluxes across different seasons, vertical levels, regions, and sample sizes.

2.3 Comparison between nitrate fluxes and primary production

We compared nitrate fluxes with new production (primary production based on assimilation of nitrate, see Dugdale and Goering (1967)) and export production. New production estimates were taken from Sakshaug (2004). Export production estimates were taken from Wiedmann (2015), who has compiled the vertical carbon export flux at 200 m depth. To enhance data coverage, we added measurements from two studies from the Central Arctic Ocean (Cai et al., 2010; Honjo et al., 2010). Details can be found in the Supplementary Material.

Both biomass and primary production are frequently given in units of carbon. To convert between units of carbon and nitrate fluxes, we employed a C:N ratio of 6.6 mol C: mol N, the so-called Redfield ratio (Redfield et al., 1963). This particular choice of C:N ratio may be criticized on the grounds that it varies depending on the type of organic matter and other environmental factors (Brzezinski, 1985; Tamelander et al., 2013), and that C:N ratios observed in the Arctic in particular are usually higher (Frigstad et al., 2014). However, turbulence measurements come with a much larger margin of error, with one detailed study giving the systematic bias between two different sets of microstructure probes, signal processing, and calibration procedures as within a factor of 2 (Moum et al., 1995). This is impressive for microstructure measurements but significantly larger than the precision with which the C:N ratio is frequently discussed in biogeochemical contexts. Therefore, by assuming a standard, constant C:N ratio, we make our results easy to adapt to other ratios should the reader want to change this number.

3 Results

3.1 Seasonal cycle of surface nitrate concentration

Winter surface nitrate concentrations in the Atlantic sector reached high values around 11 μM (Fig. 1). In the Central Arctic Ocean, concentrations stayed constant at roughly 1-3 μM throughout the year, whereas in the coastal Beaufort Sea they occasionally reached intermediate values in winter. Most regions of the Arctic however became nitrate limited ($<1\mu\text{M}$) during the summer, with the exception of the Eurasian Basin, the Makarov Basin, and some regions in Southern Fram Strait.

3.2 Nitrate fluxes

Nitrate flux estimates are still scarce given that they require co-located measurements of both turbulence and nitrate concentrations; however, they approach Pan-Arctic coverage (Fig. 2). Highest values ($> 1 \text{ mmol N m}^{-2} \text{ d}^{-1}$) were found in the Atlantic sector. The lowest values ($<< 0.1 \text{ mmol N m}^{-2} \text{ d}^{-1}$) occurred in the central basins (Canada Basin) and in Young Sound and the Laptev Sea, two locations strongly impacted by terrestrial freshwater.

3.3 Nitrate flux seasonality

The seasonal cycle of surface nitrate concentration was also reflected in its upward fluxes (Fig. 3). In areas where the water column overturned in winter, summer fluxes were an order of magnitude below winter values. A notable exception was observed at one station in the Barents Sea south of the polar front (Wiedmann et al., 2017), where the water was weakly stratified even in summer and hence nitrate fluxes were probably at least as high as in winter with 5 $\text{mmol N m}^{-2} \text{ d}^{-1}$ (Table 1), although sample size ($N=1$) was not sufficient to draw further conclusions.

Observations over a full seasonal cycle were only available in areas where the water column overturns, notably in the Barents sea and shelf slope area (Table 1). In contrast, in the non-overturning regions, fluxes were lower overall, but there is not enough data to test whether the seasonality itself is, in relative terms, really much weaker there.

4 Discussion

4.1 Nitrate fluxes as a function of stratification and seasonality

The vertical nitrate flux (F_N) in winter was remarkably well correlated with the pre-bloom nitrate surface concentration $[\text{NO}_3^-]_0$ (Fig. 4A). A linear model $[\text{NO}_3^-]_0 = 7.6\mu\text{M} + 3.4\mu\text{M} \cdot \log_{10}(F_N/\text{mmol N m}^{-2} \text{ d}^{-1})$ yielded an adjusted $R^2=0.85$ and $p=0.002$ for the linear coefficient. Consequently, deep winter mixing, where it occurs, likely is a controlling factor of the annual nitrate inventory, expanding on direct measurements of a full annual cycle over the Barents Sea shelf break (Randelhoff et al., 2015). Our results quantitatively support the perception that vertical nitrate fluxes explain the seasonality of the upper ocean nitrate inventory, as has been surmised multiple times in the literature (see e.g. Carmack and Wassmann, 2006; Tremblay et al., 2015) based on general considerations of stratification and bathymetry.

Stratification and bathymetry also governed pre-bloom surface nitrate concentrations (Fig. 4B) and, by extension from the aforementioned, vertical nitrate fluxes. Stratification represents the

resistance of the water column against overturning and vertical mixing, making its link to vertical nitrate fluxes explicit. As for bathymetry, locations with the same strength of upper-ocean stratification had on average consistently highest pre-bloom nitrate over the shelf slope ($200\text{ m} < \text{depth} < 1500\text{ m}$), lower on the shelves ($< 200\text{ m}$), and lowest over the basins ($> 1500\text{ m}$). These findings correspond to general expectations as rough or shallow topography lets currents interact with the bathymetry. Mixing in the Arctic has indeed been found to be especially elevated over the shelf slope (Rippeth et al., 2015). Tidal velocities are generally higher over the shelves than over the deep basins (Kowalik and Proshutinsky, 2013). The Arctic boundary current close to the shelf break may also provide opportunities for localized upwelling through interaction with topography or wind (Carmack and Chapman, 2003; Kämpf and Chapman, 2016).

4.2 Primary production constrained by nitrate fluxes

4.2.1 Annual basin-scale productivity

Nitrate supply should constrain primary production. Regenerated production is a large if not dominant fraction of primary production where nitrogen is scarce and is therefore not directly related to nitrate fluxes, unlike new production, which relies on nitrate brought up from below the photic zone (Dugdale and Goering, 1967). In the absence of significant advection, new production is even stipulated to be similar to the upward nitrate flux based on conservation of mass alone (see Appendix, Fig. 9).

On annual time scales, both the upward nitrate flux in winter into the surface mixed layer, the particle export at 200 m depth, and new production (nitrate uptake) matched up reasonably well for Baffin Bay, the Barents Sea, the Southern Beaufort Sea, and the Central basin (Fig. 5), both in regional patterns and order of magnitude. (Other regions lack estimates of the winter nitrate flux.) Indeed, annual budgets have to be closed if nitrate inventories are not to change in the long term. The relatively minor differences between export production, new production, and the vertical nitrate flux may reflect the extreme disparity of spatial and temporal scales of the different measurements. However, no study has systematically investigated all three quantities on annual to interannual time scales and at the same location.

4.2.2 Short-term new production

A different matter is whether or not during summer, upward mixing of nitrate limits the amount of new production in the short term. Here, the published literature gives a less clear picture (Fig. 6A). Randelhoff et al. (2016) measured vertical nitrate flux and new production for both spring and summer in the marginal ice zone around northern Fram Strait. In spring, new production was considerably larger than vertical nitrate supply as nitrate was not yet depleted and hence did not limit photosynthesis. In summer, on the other hand, when the surface water was nitrate-depleted, new production was an order of magnitude *smaller* than nitrate supply, contrary to the hypothesis.

A likely contribution to this discrepancy was the seasonal buildup of dissolved organic nitrogen (Fig. 6B) observed during the same field campaigns by Paulsen et al. (2018). The nitrate uptake rate measurements by Randelhoff et al. (2016) only considered assimilation into the particulate pool due to methodological constraints. The simultaneous production of dissolved organic nitrogen could have diverted nitrate from the particulate to the dissolved production. However,

even if there were an imbalance between supply and uptake of nitrate, the associated change in the nitrate concentration would be slow and necessitate Lagrangian measurements over weeks to detect them. Recycling of nitrogen in the microbial loop may turn out to be important when balancing nutrient fluxes with new production over short subseasonal time scales. Nishino et al. (2018) found good agreement between upward nitrate flux, nitrate uptake, and export of particulate organic matter, based on a case study in the Chukchi sea. This may represent geographic differences in the dynamics of the system, or even in the methodology. Nishino et al. (2018) used different methods from those of Randelhoff et al. (2016), even though they neglected assimilation into the dissolved nitrogen pool as well (Shiozaki et al., 2009).

Our measurements in Young Sound, North-East Greenland (see Appendix), gave a diametrically opposed perspective: Here, vertically integrated new production was significantly above the vertical turbulent supply of new nitrate in this extremely quiescent fjord. Overall productivity in Young Sound is therefore likely limited by strong stratification and weak vertical mixing (Holding et al., 2019). Tidal mixing over the two shallow sills in concert with isopycnal mixing may contribute to overall upward nitrate supply (see e.g. Fer and Drinkwater, 2014), but terrestrial runoff may also contribute significantly to the nutrient cycling (Rysgaard et al., 2003) as nitrate concentrations in run-off water are higher than those measured in the sea surface (Paulsen et al., 2017). This scenario is likely specific to this fjord and cannot be generalized around Greenland as nitrate concentrations in Greenland Ice Sheet run-off often act to dilute surface nitrate concentrations (Hopwood et al., 2019; Meire et al., 2016).

In the same vein, but outside the Arctic Ocean, Law et al. (2001) and Rees et al. (2001) found that vertical mixing supplied only 33 % of the nitrate demand at a North Atlantic site, in agreement with a study by Horne et al. (1996) in the Gulf of Maine. Even in the Mauritanian upwelling region, nitrate fluxes in excess of $100 \text{ mmol N m}^{-2} \text{ d}^{-1}$ accounted for only 10-25% of observed net community production (Schafstall et al., 2010). More extremely, Shiozaki et al. (2011) found that one location on the continental shelf of the East China Sea “exhibited a considerable discrepancy between the nitrate assimilation rate ($1500 \text{ mmol N m}^{-2} \text{ d}^{-1}$) and vertical nitrate flux ($98 \text{ mmol N m}^{-2} \text{ d}^{-1}$)”, and they went so far as concluding that “the assumption of a direct relationship between new production, export production, and measured nitrate assimilation is misplaced, particularly regarding the continental shelf of the East China Sea”.

The scarcity of dedicated measurements that evaluate both nitrate fluxes, new production, and organic nitrogen pools at relevant space-time scales is a major impediment to evaluating the direct impact of nitrate fluxes on primary productivity in the Arctic on time scales of days. However, given the correspondence we observed between new production and vertical nitrate supply over annual Pan-Arctic scales, any mismatch between the two on sub-seasonal time scales may be caused by asynchronous evolution of the different nitrogen pools (Figs. 6, 9B). Phytoplankton growth responses may also lag nutrient supply pulses, perhaps necessitating time series approaches when studying scales as short as weeks (Omand et al., 2012).

4.3 Nitrogen limitation of primary production

Nitrogen scarcity plays a large role in constraining Arctic marine primary production (Moore et al., 2013; Tremblay et al., 2015). Nutrient limitation of phytoplankton growth is usually quantified in terms of a *half-saturation constant* (of a Michaelis-Menten kinetics), above which

nutrient uptake rates benefit less and less from increasing ambient nutrient concentrations. Reported values of such half-saturation constants vary widely according to species and physiological state, but reasonable values usually range around orders of magnitude from 0.1 to 10 μM , but clustering around 1 μM (e.g. Eppley et al., 1969), with larger ones for larger cells (Chisholm, 1992) and values in the lower end for picophytoplankton (Agawin et al., 2000; Cochlan and Harrison, 1991). We infer that larger (usually bloom-forming) species are nitrate-limited in summer across large swaths of the Arctic, but not including some of the central basin, where summer surface concentrations are in excess of e.g. 5 μM in the Makarov and Nansen basins (Fig. 7). These high nitrate concentrations in the Central Arctic are usually taken to indicate regionally important light limitation by perennial sea ice cover (Codispoti et al., 2013).

A cautionary remark is in order regarding nitrate concentrations as indicators of potential growth. Since the nitrate supply, like phytoplankton growth, is a rate and not a stock, its present-day inventory alone does not yield sufficient information to infer possible limitations in future scenarios. Therefore the summer surplus nitrate observed in the central AO may only be available transiently while the ice cover shrinks, but not in a steady-state situation without summer sea ice.

In other words: If fall blooms are due to upward mixing of new nitrate, they increase new production in the short term. Whether such increases are long-term or if they instead serve to deepen the nitracline depends on the vertical mixing in winter. Similarly, a lengthening ice-free season or a more transparent ice cover lead to a deeper euphotic zone and could enhance growth in subsurface waters, richer in nutrients, but the resupply rate of nitrogen ultimately decides about potential lasting increases in new production.

4.4 Future scenarios

Randelhoff and Guthrie (2016) provided estimates of end-of-century new production, given presently observed turbulence and potential future increases in the freshwater inventory observed in a numerical circulation model (Nummelin et al., 2015). They concluded that a potential increase in new production in the Amundsen Basin (if the system were to turn to nitrate limitation) may fall victim to future increases in vertical stability. Little is known about the future of seasonal and especially summertime stratification in the surface layer (Randelhoff et al., 2017).

Contrarily, Polyakov et al. (2017) posited that an ongoing Atlantification will lead to deeper winter convection in the Eurasian Basin. As Atlantic Water is also the principal source of heat in the Arctic Ocean, it has been implicated in recent sea ice loss (Ivanov et al., 2016; Polyakov et al., 2017), and hence could regionally relieve nutrient and light limitation at the same time (Randelhoff et al., 2018). The recent decreases of sea ice extent in Northern Fram Strait and north of Svalbard (Onarheim et al., 2018) indicate that such a process is already well underway. The analogue may be happening in the Chukchi sea, where the Alaskan Coastal Current brings in both large amounts of heat (Woodgate et al., 2012) and nutrients (Torres-Valdés et al., 2013), but the published literature is less clear on the presence and effects of such a tentative advective borealization of the Chukchi sea.

4.5 Ice cover and wind-driven turbulence

The published literature is also equivocal on whether or not the decreasing ice cover will enhance turbulent mixing in the upper ocean. While less sea ice may enhance the input of wind energy into the ocean (Dosser and Rainville, 2016; Rainville and Woodgate, 2009), this energy may be dissipated at shallow depths due to the strong stratification (Lincoln et al., 2016). Reanalysis of conductivity-temperature depth and acoustic Doppler current profiler finestructure data has not shown trends in turbulent mixing in recent decades either (Chanona et al., 2018; Guthrie et al., 2013).

Broken-up, free-drifting sea ice in summer may enhance wind energy input into the upper ocean compared to ice-covered areas by enhancing surface roughness (Martin et al., 2016) but also decrease vertical turbulent mixing in the surface layer through the associated layer of meltwater (Randelhoff et al., 2017, 2016). Larger freezing rates, caused by increasing proportions of first-year ice, may increase upward mixing, but the potential effects on entrainment of nitrate into the surface layer has to our knowledge not been systematically studied. A major uncertainty in any future prognoses is the scarcity of large-scale surveys of the ice-ocean boundary layer.

4.6 Arctic nitrate fluxes in a global context

Based on a literature review (Table 2), Arctic vertical nitrate fluxes tend to be approximately one order of magnitude lower than in the rest of the world ocean (Fig. 8). Even though study sites in the global ocean may be biased by measurements seeking to explain high biological productivity (most often as the result of strong mixing and upwelling), there is a considerable difference between new production in the Arctic Ocean and the world's most productive areas.

5 Conclusions

5.1 Summary

1. Determining nitrate fluxes is a laborious task. With measurements accumulating through the last 10 years, we are now approaching a Pan-Arctic baseline. In individual regions however, seasonal coverage remains patchy.
2. Arctic nitrate fluxes are, on average, one to two orders of magnitude smaller than those observed elsewhere in the world ocean.
3. The spatial patterns of the upper ocean nitrate inventory in the Arctic are well explained by vertical nitrate fluxes.
4. On annual timescales, nitrate fluxes are a powerful tool to constrain export fluxes and new production, both of which are hard to measure autonomously.
5. On weekly or shorter timescales, the relation between nitrate supply and new production is unclear, mostly due to lack of appropriate time series data. A certain asynchronicity between the different nitrogen pools may confound budget calculations.

5.2 Avenues for further research

Besides further aggregate scale (seasonal or basin-scale) measurements of the turbulent vertical nitrate flux, two avenues emerge from our conclusions.

1. Advances in turbulence-ecosystem coupling will require dedicated or autonomous sampling and time series. Purely physics-oriented turbulence sampling often does not sufficiently resolve the biologically relevant surface layer.
2. Prediction of upper ocean mixing and ice-ocean interaction depends on sea ice melt and freeze rates, expressed as buoyancy fluxes or in units of meters of freshwater equivalent per unit area. Yet, to our knowledge, this quantity is not routinely investigated as output of coupled ice-ocean circulation models and so no such data product exists that could aid in the extrapolation of Pan-Arctic patterns of the seasonal vertical nitrate flux.

5.3 Upscaling primary production measurements

While currently publicly available datasets may be more comprehensive for new and export production than for nitrate fluxes, they possess some drawbacks concerning evaluating large-scale patterns. As incubations to determine new production are usually point measurements, averaging them is not trivial. Sediment traps, while measuring export fluxes at a single location, integrate the time dimension, and so are more representative, but also require a large logistic effort. Chemical tracer approaches (e.g. Moran et al., 2003) make the data acquisition phase easier, but still require water samples and are hence not easily amenable to autonomous exploration. In sum, current Arctic Ocean exploration does not scale well. Nitrate fluxes, on the other hand, can be estimated purely based on physical sensor data and hence with larger scope both in time and space.

Such turbulence measurements do not necessarily have to be conducted using microstructure profilers - mixing can also be estimated from current shear or density strain fine-structure with more standard instruments, which may work especially well in discerning relative magnitudes but can also be calibrated using regional microstructure estimates (Chanona et al., 2018; Gargett and Garner, 2008; Guthrie et al., 2013; Polzin et al., 2014). Parameterizations of this kind, relying on models of internal wave breaking, are most useful away from boundaries, in scenarios of perennial stratification where year-round background fluxes dominate (Randelhoff and Guthrie, 2016), and less so to characterize near-surface mixing. Other promising avenues are approaches based on turbulence structure functions (Wiles et al., 2006), high-frequency Acoustic Doppler Current Profiler measurements, or microstructure sensors deployed on moorings and gliders (Scheifele et al., 2018).

Turbulence also obeys tight physical constraints imposed by wind, tidal and other energy available for mixing, and by the freshwater (density) fluxes that cause background stratification. Nitrate fluxes may therefore be more easily constrained than plankton photophysiology that is notoriously variable across species and environmental conditions (e.g. Bouman et al., 2018).

5.4 Perspectives

This study has focused on vertical diffusive transport, largely ignoring other transport modes. Upwelling (Carmack and Chapman, 2003; Kämpf and Chapman, 2016), horizontal advection (Torres-Valdés et al., 2013), mesoscale eddy shedding (Watanabe et al., 2014), benthic processes (Renaud et al., 2015), and river biogeochemistry (Frey and McClelland, 2009) all likely affect Arctic Ocean primary production at least regionally. The fact that Pan-Arctic patterns of primary production can seemingly be explained without the need to invoke any of these mechanisms also

showcases the stark contrasts between the different Arctic regimes that likely shadow intra-regional nuances.

Mesoscale turbulence can contribute to cross-shelf transport and nutrient supply in the Chukchi sea (Watanabe et al., 2014). Some studies suggest that eddies may also contribute to cross-shelf transport along the West Spitsbergen Current (Hattermann et al., 2016). Crews et al. (2018) found eddies may contribute to ventilation of halocline waters in the European Arctic, meaning they would be apparent in the upward vertical fluxes measured out of the halocline waters instead of contributing directly to mixed-layer nitrate pools. Johnson et al. (2010), working in the Subtropical North Pacific, stressed the importance of event-driven upward nitrate transport not easily captured by vertical diffusivities, and even the possibility of immediate utilisation of nitrate in an otherwise diabatic isopycnal excursion, for example associated with a passing eddy. Attention is required summing these contributions, however, as there is a certain danger of double counting nitrate fluxes in eddies (Martin and Pondaven, 2003; Martin and Richards, 2001).

Advection with ocean currents manifests itself largely as transport with the Pacific and Atlantic currents that e.g. Torres-Valdés et al. (2013) have discussed. For the most part, these currents are subducted under local (Arctic) water masses and can hence be accounted for as part of the vertical fluxes downstream. Randelhoff et al. (2016) have argued that as these currents come from further south where primary production starts earlier and terminates later, the surface waters they carry are as nutrient-depleted as the Arctic surface waters. This argument has, however, never been tested quantitatively. Similarly, upwelling along coasts, shelf breaks, in eddies, and at marine-terminating glaciers may contribute regionally to ocean productivity (Carmack and Chapman, 2003; Kämpf and Chapman, 2016; Meire et al., 2017). Arguments as to how exactly upwelling is caused and how it impacts nutrient fluxes have largely remained qualitative (Randelhoff and Sundfjord, 2018; but see Spall et al., 2014 for a careful modelling exercise).

Lastly, turbulent mixing is much more than only the vertical nitrate flux. It affects predator-prey interactions (Kiørboe, 2008), nutrient uptake rates at the cell level (Karp-Boss et al., 1996), light exposure of individual cells (Sverdrup, 1953), etc. In fact, mixing and variability is a resource in itself that can be exploited by different plankton life strategies (Margalef, 1978). These concepts may turn out to be important in particular when interpreting regional specifics such as biological hotspots. As methods advance and measurements accumulate, we expect that more efforts can be dedicated to studying regional phenomena in a Pan-Arctic unified manner.

6 Conflict of Interest

The authors declare that the research was conducted in the absence of any commercial or financial relationships that could be construed as a potential conflict of interest.

7 Author Contributions

AR designed the study, made all visualizations, and wrote the first draft of the manuscript. AR, JMH, and MS conducted field sampling and data analysis of the Young Sound data. MBA and

442 MJ sampled and analyzed the Laptev Sea data. MB lead the acquisition of the Baffin Bay data.
443 JET contributed Canadian Archipelago nutrient data. All authors commented on the manuscript.

444 **8 Funding**

445 Data acquisition of BGC-Argo Floats in Baffin Bay was funded through the NAOS project.
446 Work in Young Sound was supported by the DANCEA project “De-icing Arctic coasts” and the
447 Greenland Ecosystem Monitoring Programme. AR was supported by the Sentinel North program
448 of Université Laval, partly funded by the Canada First Research Excellence Fund, and Carbon
449 Bridge, a Polar Programme (project 226415) funded by the Norwegian Research Council. JMH
450 was supported by the European Commission H2020 programme under the Marie Skłodowska-
451 Curie Actions (GrIS-Melt: grant no. 752325). MBA was supported by the National Science
452 Foundation (PLR-1203146 AM003) and the National Oceanic and Atmospheric Administration
453 (NA15OAR4310156).

454 **9 Acknowledgments**

455 The present paper started taking shape around the 4th “Symposium on Pan-Arctic Integration”,
456 held in Motovun, Croatia, 2017, and we thank all participants for inspiring discussions.

457 We thank Andrey Novikhin (AARI) for preparing the nutrient measurements from the Laptev
458 Sea shelf, Xiaogang Xing for quality-controlling and calibrating the Baffin Bay BGC Argo data,
459 and Jørgen Bendtsen and Torben Vang for providing Young Sound bathymetry data. We are
460 further grateful to Shigeto Nishino for clarifying discussions about his work in the Chukchi Sea.

461 Data exploration and visualization relied heavily on the [Holoviews library](#) (Stevens et al., 2015).

462 **10 Supplementary Material**

463 The supplemental material, accessible at <https://github.com/poplarShift/arctic-nitrate-fluxes>,
464 contains:

- 465 • The python code necessary to reproduce all analyses and figures, licensed under GNU
466 GPL3.
- 467 • The data, as plotted in all figures, in machine-readable formats.
- 468 • An interactive version of this article where figures can be zoomed, panned, and selectively
469 highlighted (as appropriate) leveraging the [Bokeh library](#) (Bokeh Development Team,
470 2018).

471 **11 Data Availability Statement**

472 All data that were published for the first time in this study are included with the above
473 repository. The rest are included to the extent possible.

12 Appendix

Numerous

12.1 The marine nitrogen cycle

Discussions of ocean surface nitrogen budgets center around the marine nitrogen cycle. Fig. 9 shows a simplified version adapted to Arctic conditions. The main component is the cycling between inorganic nitrate and particulate organic nitrogen (PON). Upward transport of NO_3^- compensates nitrate uptake by algae into PON (Dugdale and Goering, 1967) and subsequent sinking of this organic matter. The loop is closed by remineralization into nitrate at depth. When nitrogen is scarce in the surface layer, there is also intense recycling of nitrogen that has already been assimilated into organic matter, which is called regenerated production.

Additional complexity arises from a number of sources, sinks, and recycling processes not accounted for in this simplistic view. One of the conclusions of the present study is that we do not need to invoke those processes to understand Arctic surface layer budgets on a Pan-Arctic scale. Riverine inputs of nitrate are thought to be sufficiently small to be neglected at larger-than-regional scales (see e.g. Tank et al., 2012). Some of the produced PON is also harvested e.g. by higher trophic levels or fisheries (e.g. Valiela, 2015), although the latter process is likely only regionally important, e.g. in the Barents Sea. Other factors may be important depending on the regional scope. Advection, upwelling, and mesoscale mixing have already been discussed in the main text. Nitrification, denitrification, and nitrogen fixation are in general not well constrained in the Arctic Ocean (Blais et al., 2012; Sipler et al., 2017; Tremblay et al., 2008). Randelhoff et al. (2015), for instance, argued that winter vertical turbulent nitrate fluxes in areas with deep mixing are likely much larger than nitrification, but did so based on sparse data. A complete assessment of all these factors is beyond the scope of this paper.

12.2 The vertical layering of Arctic Ocean nitrate

Fluxes are easiest to measure across strong gradients. A given vertical profile of nitrate concentrations in the Arctic Ocean can schematically be vertically divided by two nitraclines (Fig. 9A): First, a seasonal one, which marks the transition from surface waters, modulated by seasonal freshwater from ice melt or terrestrial runoff and algal growth, to the remnant winter mixed layer. Second, and mostly present in the deep basins of the Arctic Ocean, one that we dub “perennial” as it is not eroded and re-established on an annual basis.

The seasonal nitracline may be completely mixed during winter (Fig. 9B), rendering fluxes hard to estimate using the “diffusivity times gradient” formula. Across the perennial nitracline, fluxes can be estimated year-round stipulating the seasonal variations in nitracline dissipation are minor, a method exploited by Randelhoff and Guthrie (2016) to estimate Pan-Arctic patterns of upward nitrate supply in the deep basin. In practice, the two nitraclines are often not clearly delineated. The distinctive characteristics of the two nitraclines are most easily seen in the Eurasian Basin, where deep winter mixed layers are clearly separated from underlying Atlantic Waters. In the Canadian Basin, strong stratification prevents winter mixing from penetrating deep into the nitracline (Peralta-Ferriz and Woodgate, 2015), leading to relatively small seasonal excursions in surface nutrient concentrations and a less distinct winter remnant mixed layer (Fig. 9C).

Consequently, we classified the seasonality of all vertical nitrate flux estimates discussed in this paper in terms of whether the water column mixes deeply (“overturns”) in winter or not (in which case stratification is dubbed “perennial”). We used the published literature for each location as well as the data set corresponding to the flux estimate, if available. Importantly, our classification is generally well-founded but occasionally ad-hoc and tentative due to sparse data. An illustrative example are three summertime flux estimates north of the Barents sea polar front (Sundfjord et al., 2007; Wiedmann et al., 2017). For instance, Loeng (1991) indicates a weak but persistent salinity stratification in the Arctic water mass throughout winter, but the few vertical nitrate profiles available in our compiled data set indicate a seasonal cycle of surface nitrate in line with what is seen south of the Polar Front. These three fluxes were hence classified as being in a location where the water column overturns in winter because we focused on the vertical structure of nitrate profiles. Either way, because all three fluxes were based on a small sample size, not too much weight was given to them in the overall analysis.

12.3 Measuring vertical nitrate fluxes

Barring regionally important processes such as upwelling and eddy pumping (Carmack and Chapman, 2003; Kämpf and Chapman, 2016; Randelhoff and Sundfjord, 2018), the most prevalent form of the upward transport of nitrate in the ocean is turbulent diffusion (Lewis et al., 1986). Such diffusion mixes the spent surface waters with deeper, more nutrient-rich waters, thereby replenishing their nitrate reservoir. A vertical turbulent nitrate flux is, by definition, the product of a so-called “diapycnal eddy diffusivity” with the vertical gradient of nitrate. This is completely analogous to any other tracer such as temperature or salinity. The interested reader is referred to the vast literature on turbulent flows.

To estimate both those quantities, one has to measure the turbulence and a vertical profile of nitrate concentrations at the same time and location. Determining nitrate concentrations is comparatively uncomplicated because only the non-turbulent background is needed; one can use either bottle samples or, preferably, optical nitrate sensors to achieve a better vertical resolution (Alkire et al., 2010; Randelhoff et al., 2016). Both of these options are easily integrated into standard sampling with a CTD rosette. While care should be taken to calibrate the absolute concentrations of optical sensors against water samples, such biases are usually depth-independent and hence do not matter for the calculation of the gradients (see Appendix of Randelhoff et al., 2016). Measuring turbulence is more challenging because it requires either measurements with sophisticated instruments, requiring dedicated ship time and personnel, or parameterizations that add layers of uncertainty (e.g. Garrett and Munk, 1975; Guthrie et al., 2013).

12.3.1 Measuring turbulence

The most direct way of determining a nitrate flux is measuring the so-called “dissipation of turbulent kinetic energy” (ϵ) traditionally using free-falling microstructure profilers (Lueck et al., 2002). ϵ can also be estimated from finescale current shear (i.e. current profiles) or strain visible in CTD profiles (Guthrie et al., 2013). Once ϵ is determined, its accuracy usually cited as being within a factor of two (Moum et al., 1995), the vertical turbulent diffusivity can be calculated, following Osborn (1980), as

$$K_\rho = \Gamma \frac{\epsilon}{N^2} \quad (1)$$

where N^2 is the Brunt-Väisälä buoyancy frequency and $\Gamma \approx 0.2$ is the mixing coefficient that reflects how much of ϵ is available for adiabatic mixing. Eq. 1 has a number of known issues, a major one being that Γ is not constant. A variety of different parameterizations have been proposed (e.g. Shih et al., 2005; Bouffard and Boegman, 2013), with no clear alternative emerging. Eq. 1 is hence the de facto standard (Gregg et al., 2018), and in fact all turbulence-based estimates of the vertical nitrate flux compiled for this paper are based on it. Most often, $\Gamma = 0.2$ is used, but e.g. Sundfjord et al. (2007) used $\Gamma = 0.12$ following recommendations in the literature consistent with their dataset (see references therein).

12.3.2 Using the inorganic nitrate drawdown as an indicator of nitrate flux

Another method to determine vertical nitrate fluxes, less direct, uses a set of nitrate profiles through fall and winter (Randelhoff et al., 2015). It has been employed to calculate two of the fluxes presented in this study. Vertically integrating the successive differences between them, one essentially reverses the calculation of net community production by the nitrate drawdown between winter and summer (Codispoti et al., 2013). Randelhoff et al. (2015) provided a brief overview over potentially interfering processes such as nitrogen fixation (Blais et al., 2012) and concluded they were likely not significantly disturbing the annual budgets, but it has to be acknowledged that data is sparse. While this method may be robust in the pelagic, one can doubt its effectiveness in waters where nitrogen cycling is heavily affected by other processes, such as benthic processes in shallow waters, or coastal effects.

12.4 New estimates of nitrate fluxes and new production in Young Sound, NE Greenland

12.4.1 Methods

Sampling in the Young Sound/Tyrolerfjord system was conducted during three weeks in August 2015 from the Daneborg research station as part of the Danish MarineBasis program in Zackenberg (Fig. 10A).

Water column nutrient samples were taken at 5 stations using a manually operated Niskin bottle from depths of 1, 5, 10, 20, 30, 40, 50, and 100 m. They were filtered with Whatman GF/F filters before being stored in previously acid-washed 30 mL high-density polyethylene (HDPE) plastic bottles and frozen until analysis (-18 °C). Nitrite (NO_2) and nitrate (NO_3^-) concentrations in each sample were measured on a Smartchem200 (AMS Alliance) autoanalyzer.

An MSS-90L (Sea and Sun Technology, Germany) free-falling microstructure profiler was deployed at a total of 37 stations, many of them repeat stations, to measure vertical profiles of the dissipation of turbulent kinetic energy. At the same stations, we deployed a SUNA (Satlantic) nitrate spectrophotometer to collect co-located vertical profiles of nitrate concentration. SUNA profiles were post-processed following (Randelhoff et al., 2016) and calibrated using a constant bias determined from comparison with the nutrient water samples.

New and regenerated production were investigated at a subset of five stations. They were measured in two parallel incubations, labelled with ca. 10% ambient concentration of $^{15}\text{NO}_3^-$ and $^{15}\text{NH}_4^+$ respectively. Water samples were incubated in triplicate 500 ml polycarbonate bottles in situ. Additionally ca. 10% ambient concentration of ^{13}C -bicarbonate was added to both sets of incubations to follow the incorporation of inorganic carbon into biomass. Samples were taken for $\text{NO}_2^- + \text{NO}_3^-$, $^{15}\text{NO}_3^-$ and $^{15}\text{NH}_4^+$ before and after addition of tracers by filtering through a syringe

filter (Whatman GF/C) into 10 ml polystyrene vials which were frozen (-18 °C) until analysis. After the incubation the particulate matter from each incubation vessel was filtered onto pre-combusted GF/F filters and later the ^{15}N and ^{13}C content of the particles on the filters was determined by mass spectrometry. Before filtration a third set of samples for $\text{NO}_2^- + \text{NO}_3^-$, $^{15}\text{NO}_3^-$ and $^{15}\text{NH}_4^+$ were taken. $\text{NO}_2^- + \text{NO}_3^-$ was determined photometrically following Schnetger and Lehnert (2014). $^{15}\text{NH}_4^+$ was determined based on Risgaard-Petersen et al. (1995). $^{15}\text{NO}_3^-$ was determined as in Kalvelage et al. (2011). New and regenerated production were calculated as the ratio of nitrate or ammonium to total N-uptake in each incubation respectively multiplied by the total C-uptake in each incubation.

In total, we collected 43 profiles of co-located SBE25+SUNA profiles, 103 MSS casts, 40 nutrient bottle samples and 20x3 triplicates of new and regenerated production incubations.

12.4.2 Results

A freshwater layer was present throughout the fjord, but most prominent in the innermost parts (Fig. 10B-D). Nitrate was depleted throughout the upper 40 m, below which concentrations steeply rose to about 4 μM . The fjord was remarkably quiescent in terms of turbulent dissipation rates, but mixing was significantly elevated over the sills. Vertical nitrate fluxes, computed for each station of co-located MSS and SUNA measurements, ranged from 0.012 to 13.26 $\text{mmol N m}^{-2} \text{d}^{-1}$, with some of the values in the fjord interior being the lowest observed across this entire study. Median upward fluxes were 0.036 and 0.33 $\text{mmol N m}^{-2} \text{d}^{-1}$ in the fjord interior and over the sills, respectively. Incubations, although only available at two depths (5 and 20 m), indicated new production rates on the order of 0.1 to 1 $\text{mmol N m}^{-2} \text{d}^{-1}$ (Fig. 10E).

12.5 Nitrate flux estimate in the Laptev Sea

12.5.1 Data description

Microstructure and nutrient measurements from the Laptev Sea were collected under the framework of the German-Russian “Laptev Sea System”-partnership in winter 2008 and the summers of 2011, 2014, and 2018 (Fig. 11B). The 2008 profile was averaged from measurements collected during the helicopter-supported “Transdrift 13” winter expedition (6 April to 10 May 2008) to the southeastern Laptev shelf. The summer nitrate profile was averaged from profiles collected during the “Transdrift 19” expedition on board the RV Jakov Smirnovsky in September 2011 (Bauch et al., 2018).

In 2014 microstructure turbulence profiles were collected on 19 September 2014 during the Transdrift 22-expedition aboard the RV Viktor Buinitsky (see Janout et al., to be submitted to this issue). The dissipation rates of turbulent kinetic energy (ϵ) were derived from shear variance measured with a freely falling MSS-90L microstructure profiler manufactured by Sea and Sun Technology (SST, Germany). Vertical profiles of epsilon were calculated from the isotropic formula and spectral analysis of 1-s segments and subsequently averaged into 1-m bins. Turbulent vertical fluxes are based on a diapycnal eddy diffusivity with a constant mixing efficiency taken to be 0.2 (Osborn, 1980). For statistical robustness, the 2014 MSS profile shown in this paper was averaged from a series of five casts.

In 2018 a joint German-US-Russian expedition to the Eurasian Arctic was carried out aboard the RV Akademik Tryoshnikov from 18 August to 30 September 2018. The expedition combined the

German-Russian CATS (Changing Arctic Transpolar System) and the US-Russian NABOS (Nansen Amundsen Basin Observing System) programs. The dissipation profile was again generated with a MSS-90L, while the nitrate profile was recorded with a Deep SUNA V2 nitrate profiler (Seabird Scientific) attached to the shipboard CTD/rosette. These data files were then processed using a program (ISUSDataProcessor) developed by Ken Johnson (MBARI) that corrects the spectral data for temperature effects on the bromide absorption and applies a linear baseline correction to account for absorption by colored dissolved organic matter (Sakamoto et al., 2009). SUNA nitrate concentrations were then compared with nitrate concentrations measured from discrete seawater samples collected at various depths above 20 and below 300 m depth where concentrations were sufficiently constant with depth. The full description of the methods is distributed with the data (Alkire, 2019).

12.5.2 Nitrate fluxes

Two representative profiles were selected to compute nitrate fluxes (Fig. 11A): Cast 59 and a co-located MSS profile, both sampled in 2018, and the 2014 MSS profiles and cast 62, also co-located but from separate years. For both profiles, we visually determined the nitracline, averaged ϵ over that interval, and computed the average nitrate and density gradients by a linear regression. The resulting nitrate fluxes were 0.014 and $0.017 \text{ mmol N m}^{-2} \text{ d}^{-1}$, and hence we entered the average value of $0.015 \text{ mmol N m}^{-2} \text{ d}^{-1}$ for the Laptev Sea into the nitrate fluxes compilation.

Even though we have a winter and a summer vertical profile of nitrate concentrations, we cannot calculate a winter flux using the integrated drawdown (Codispoti et al., 2013; Randelhoff et al., 2015) because comparison of the winter and summer profiles does not indicate any reliable vertical structure in the drawdown. This may indicate that winter fluxes might be too small to make a noticeable difference between the summer and winter profiles. More importantly, in such a shallow shelf sea, other factors (such as benthic nitrogen cycling or riverine freshwater) may also play a role as detailed above.

12.6 Nitrate flux estimate in Baffin Bay

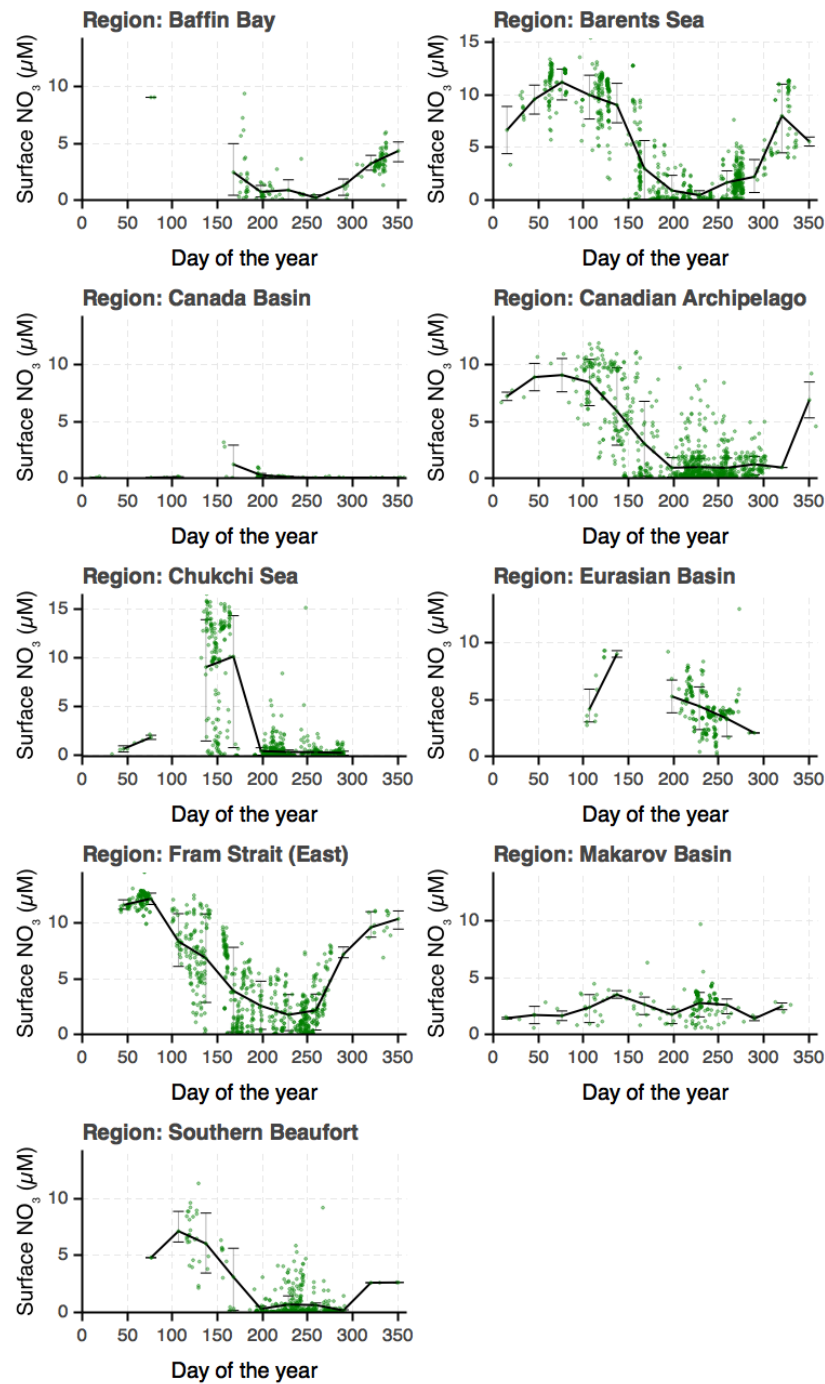
Three biogeochemical Argo floats, part of the NAOS project, overwintered in Baffin Bay from July 2017 to July 2018, described in detail by Randelhoff et al. (2020, in prep.).

Nitrate concentration was observed by the Satlantic Submersible Ultraviolet Nitrate Analyzer (SUNA). Each sensor's offset, taken to be constant and depth-independent (Randelhoff et al., 2016), was corrected based on nitrate concentration profiles sampled during deployment of the floats. Mixed layer depth was defined as the shallowest depth where density rose more than 0.1 kg m^{-3} above the surface density.

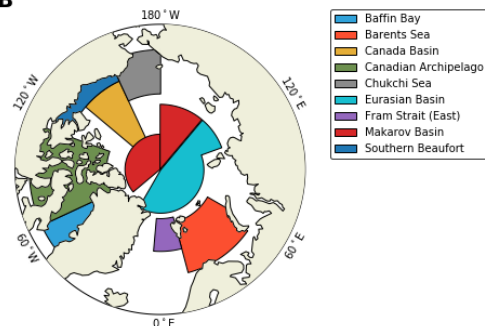
Integrating the nitrate deficit $\Delta[\text{NO}_3^-] \equiv [\text{NO}_3^-](60\text{m}) - [\text{NO}_3^-](z)$ over the upper 60 meters for each station shows that over the course of four months (from November to March), a deficit of $200 \text{ mmol N m}^{-2}$ was replenished, approximately equivalent to an upward nitrate flux of $1.66 \text{ mmol N m}^{-2} \text{ d}^{-1}$ (Fig. 12). Although each float was drifting during the course of the winter, which may have introduced advective changes, the floats were well dispersed across Baffin Bay and should give a representative picture of winter mixed layer evolution. Details are deferred to the aforementioned manuscript (Randelhoff et al., in prep.). The usual caveats about neglecting

680 mixed-layer regeneration and consumption of nutrients apply, and so this calculation makes the
681 same kind of assumptions as have been detailed by Randelhoff et al. (2015).

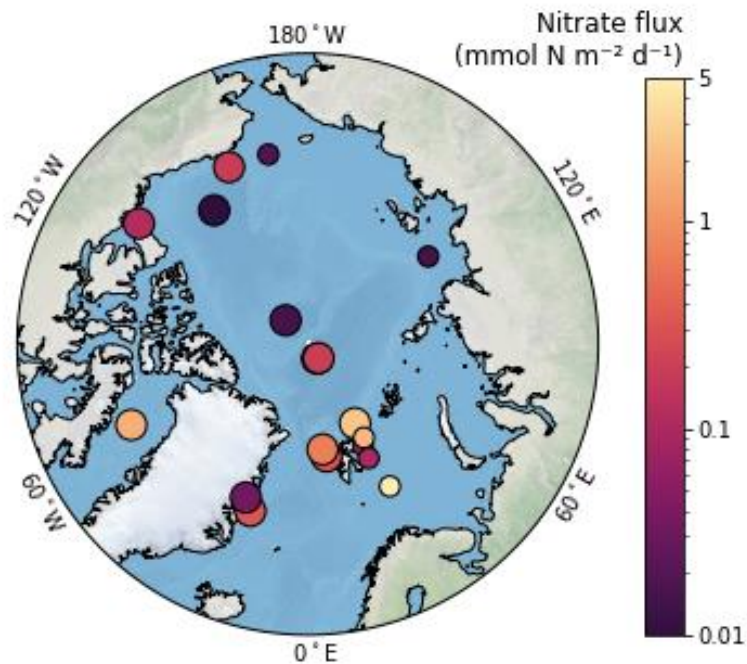
A



B



684 *Figure 1: (A) Seasonal cycles of surface nitrate concentrations in different regions of the*
685 *Arctic. (B) The delineation of these regions largely follows Codispoti et al. (2013) and Peralta-*
686 *Ferriz and Woodgate (2015).*



687
688 *Figure 2: All nitrate flux compilation across the AO compiled for this study, irrespective of*
689 *season and vertical levels. The smaller dots indicate single stations, whereas the big dots*
690 *represent averages over larger time or space scales.*

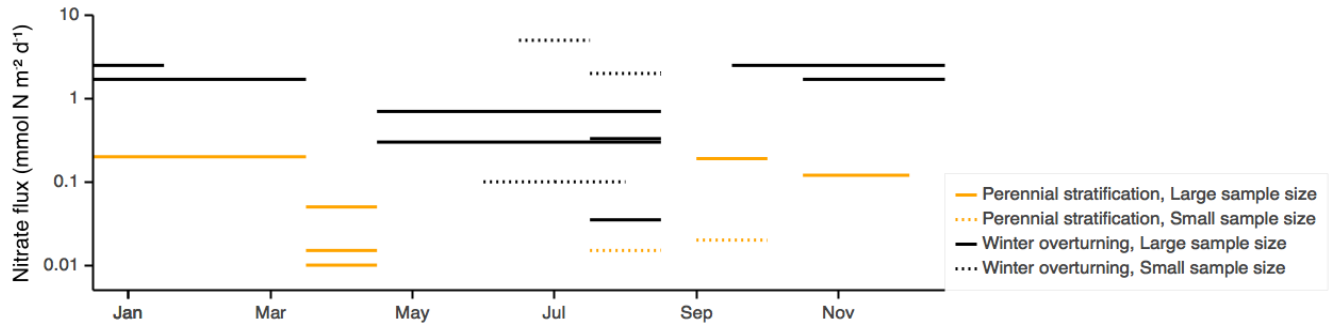


Figure 3: Vertical turbulent nitrate fluxes as a function of the month. Black lines mark the regions where the water column overturns in winter and orange those where it does not. Dotted lines reflect flux estimates based on small sample sizes (N), potentially not very representative of the regional or seasonal scale, whereas solid lines indicate data that are representative of a larger spatial or temporal scale.

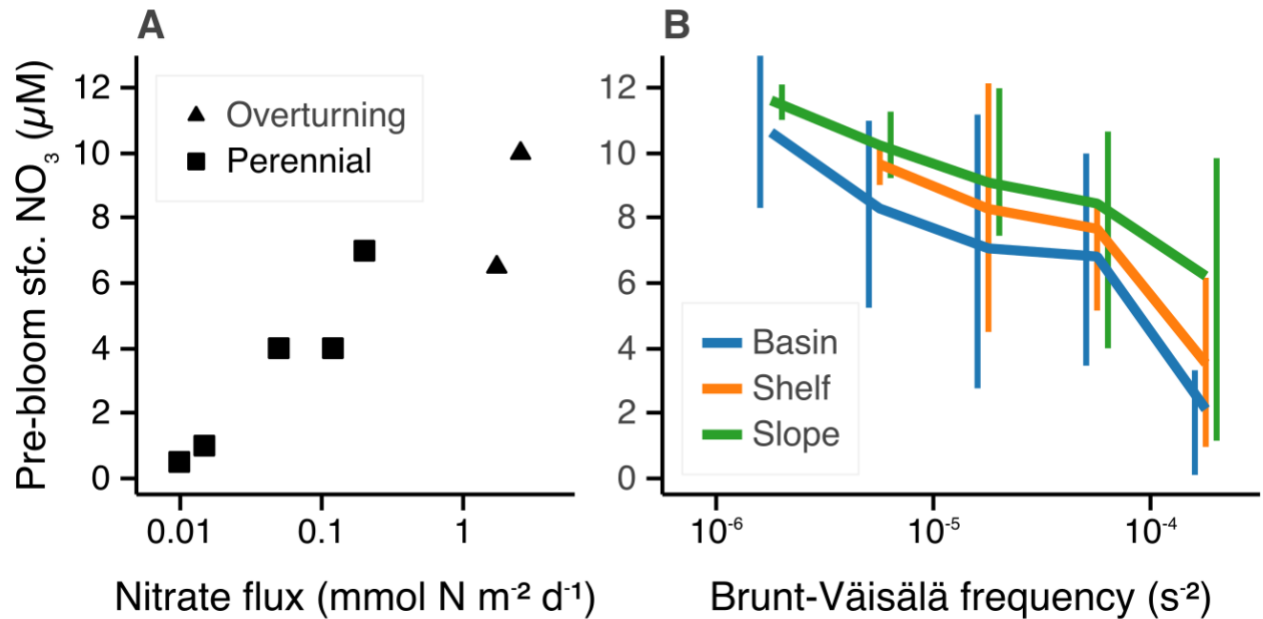


Figure 4: The surface nitrate inventory dominated by variations in turbulent mixing. The annual pre-bloom surface nitrate concentration graphed as a function of (A) the vertical nitrate flux during winter and (B) the strength of water column stratification in the upper 30-60 m depth interval. The bold curves show average nitrate concentration for a given strength of stratification for either of three bathymetry types. Vertical bars (horizontally slightly offset to increase readability) indicate the standard deviation of data for each bin. Data sources: (A) nitrate flux compilation, (B) nitrate profile database.

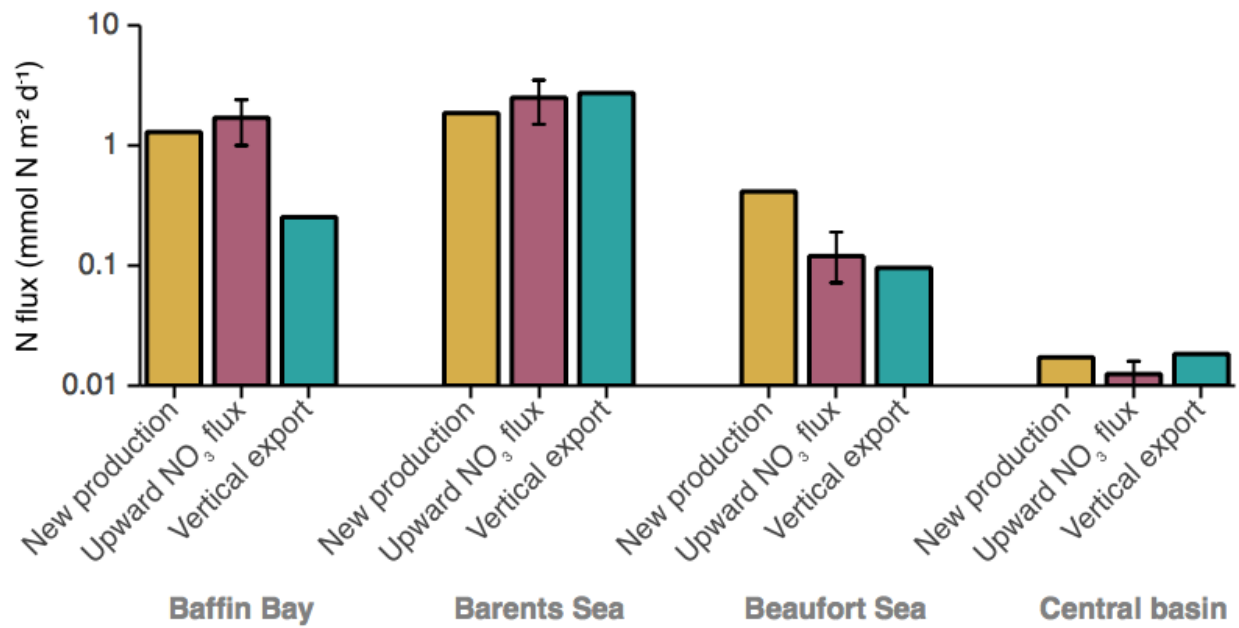


Figure 5: Annual nitrogen fluxes in the Arctic surface ocean. Winter average upward nitrate flux, new production, and vertical downward particle export (converted to nitrogen units using the Redfield ratio) at 200 m depth compared across four regions of the Arctic Ocean. Data sources: Nitrate fluxes, see Table 1; new production, Sakshaug (2004); export production, Wiedmann (2015), Honjo et al. (2010), and Cai et al. (2010). Error bars were systematically only available for nitrate fluxes.

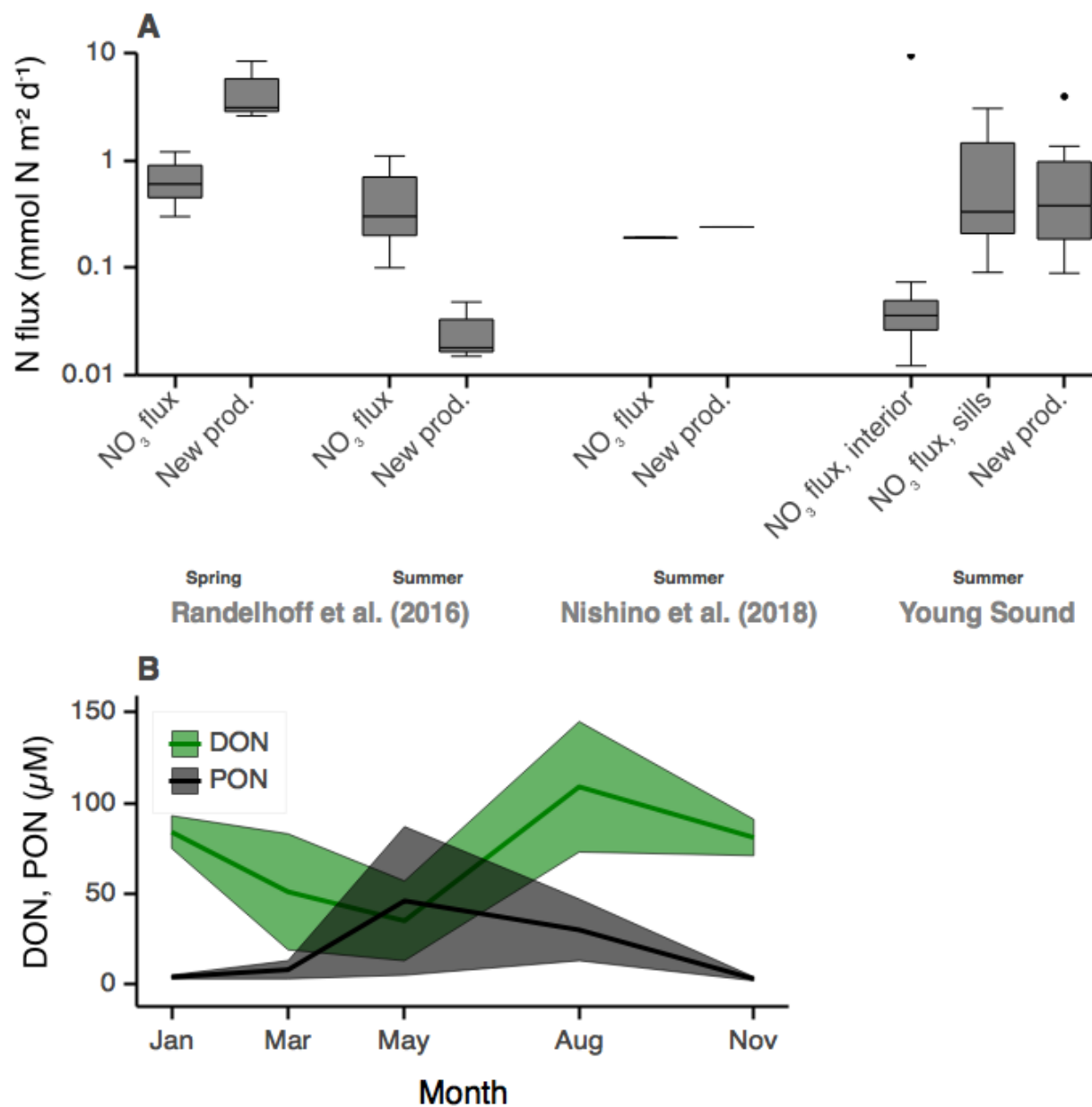
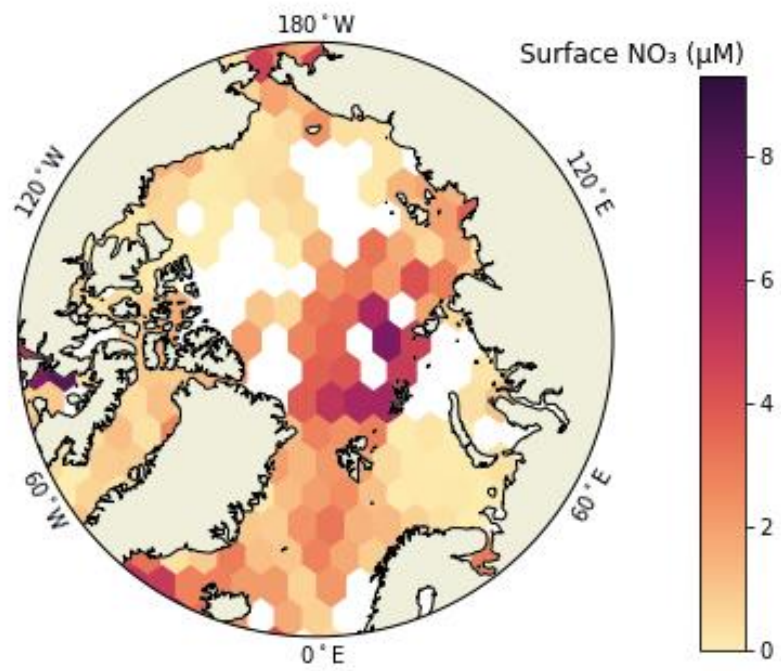
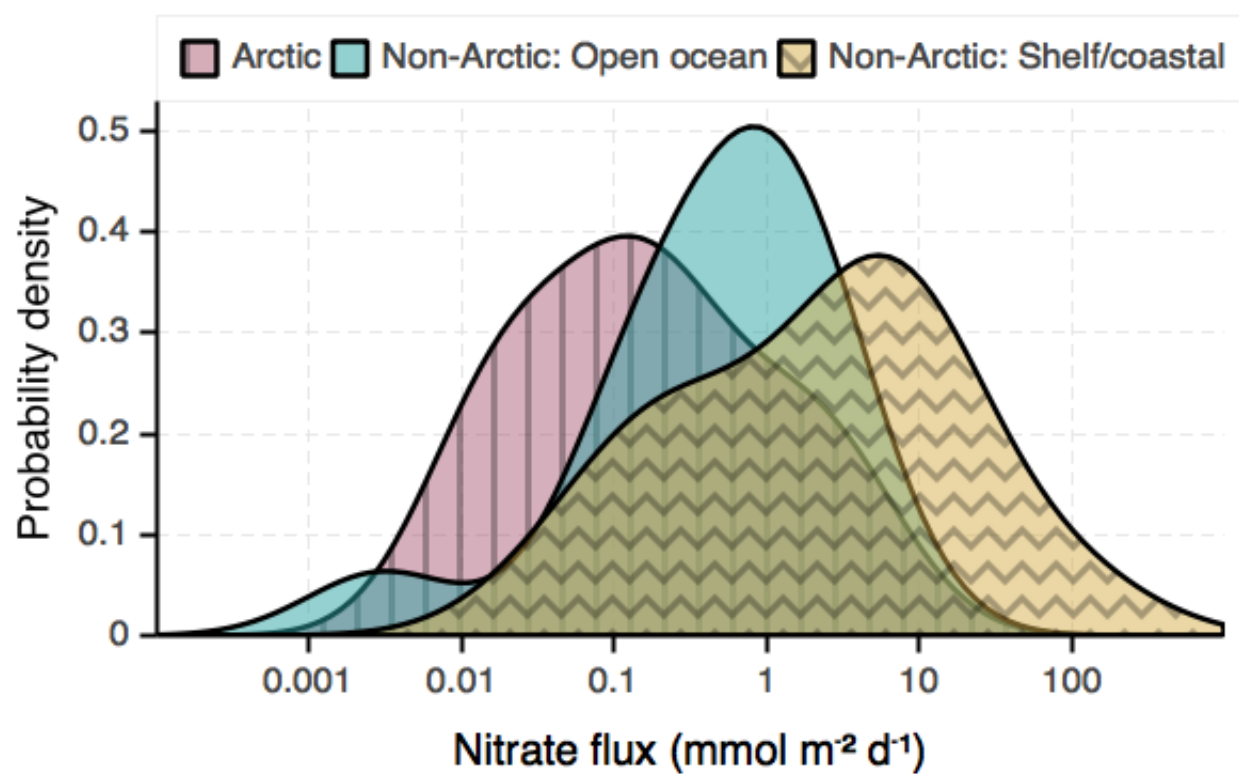


Figure 6: (A) New production incubations compared with upward nitrate flux for three case studies. Data sources: Randelhoff et al. (2016), Nishino et al. (2015), this study (see Appendix). (B) Annual cycle of dissolved (DON) and particulate organic nitrogen (PON) observed in the seasonal ice zone of Fram Strait. Shaded areas indicate the standard deviation. Data source: Paulsen et al. (2018), their Table 1.



718

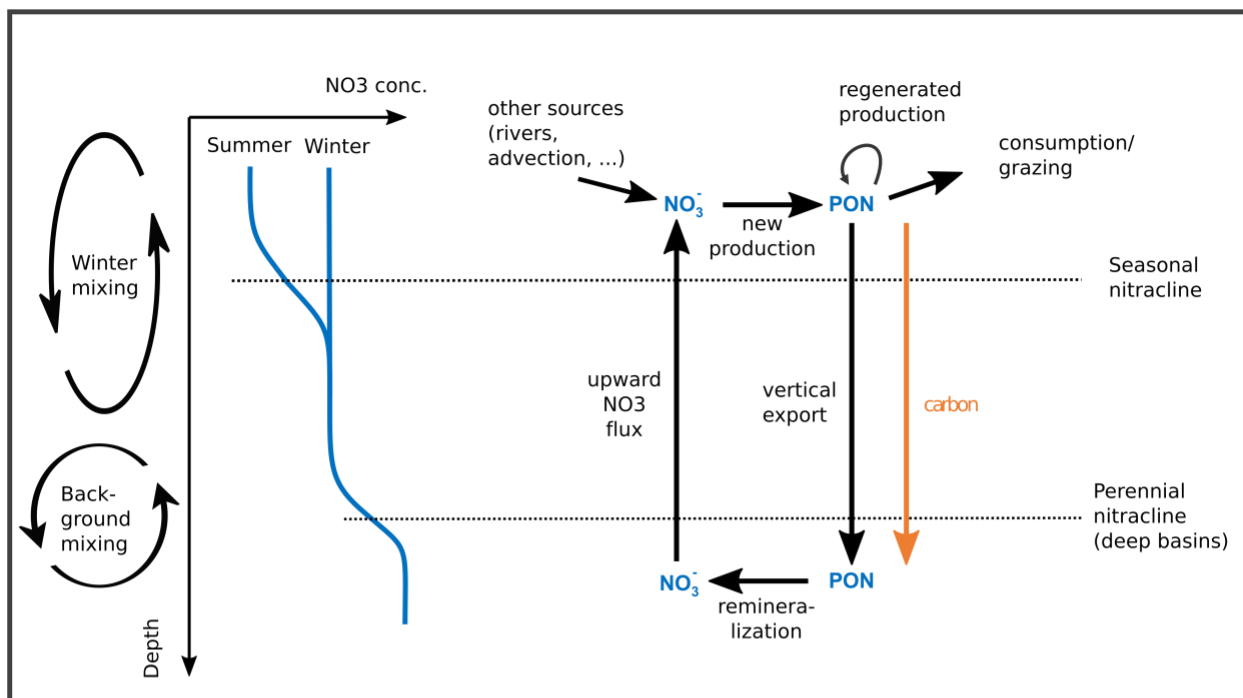
719 *Figure 7: Summer surface nitrate concentration.*



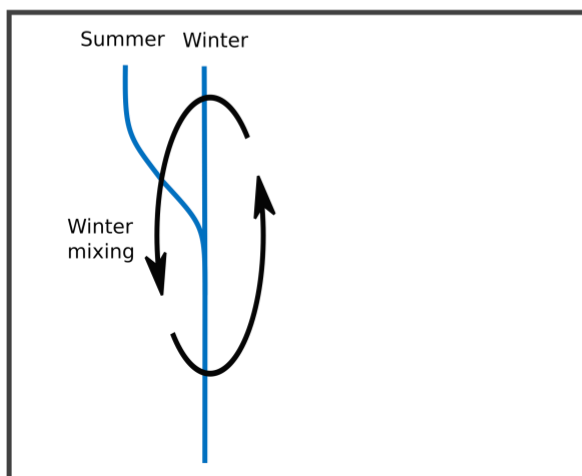
720

721 *Figure 8: Distributions (kernel density estimates) of observed nitrate fluxes based on Tables 1*
 722 *and 2. Note that these curves give each observation the same weight, regardless of areal or*
 723 *temporal scope.*

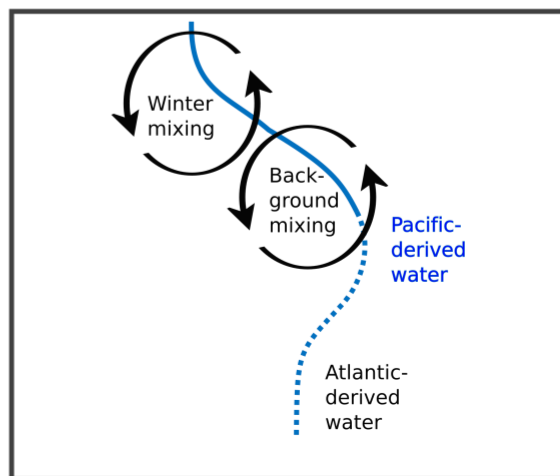
A: General scheme (e.g. Amundsen Basin)



B: Seasonal stratification/ winter overturning (e.g. Barents Sea, Baffin Bay)



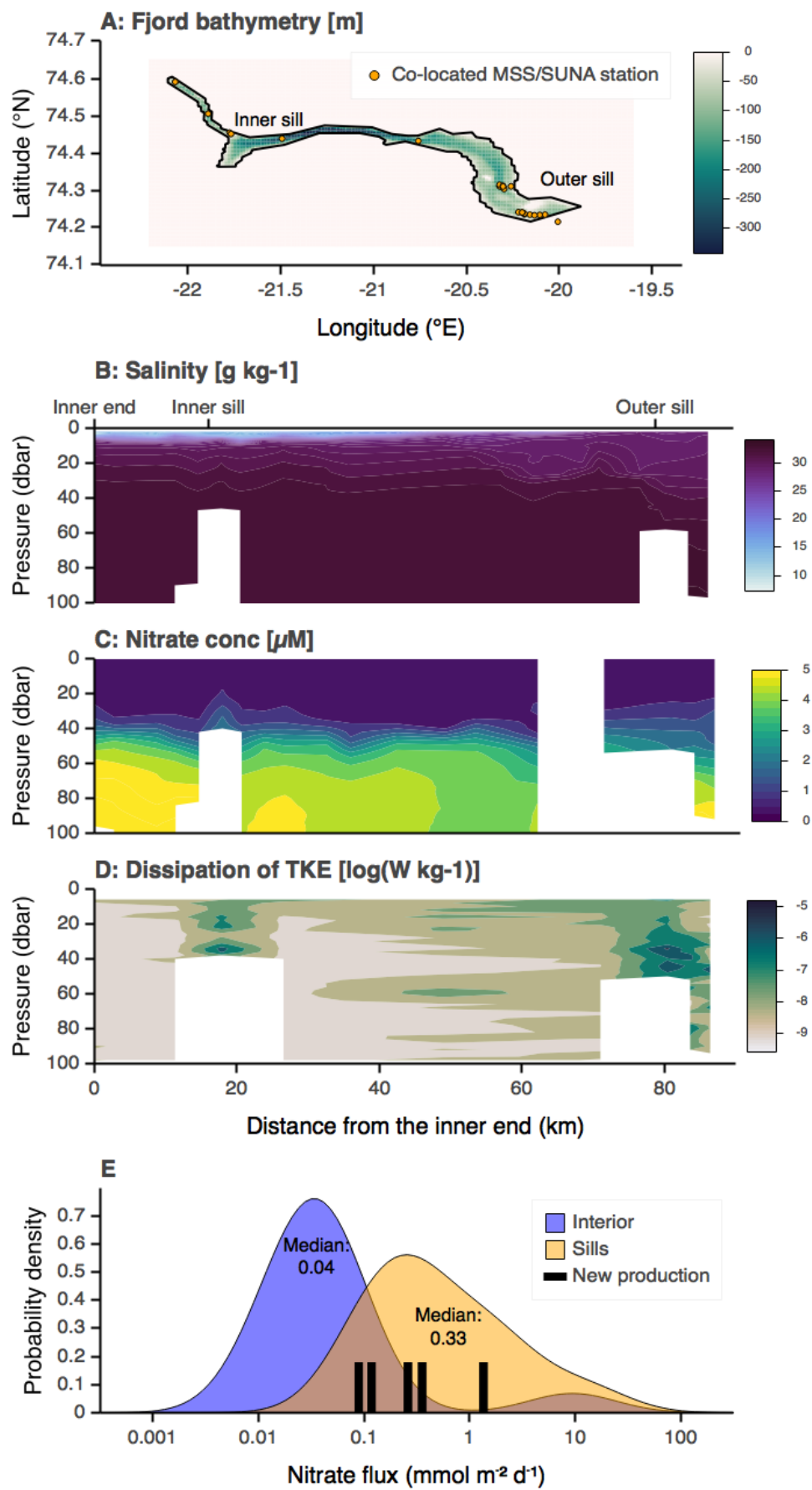
C: Perennial stratification: Seasonal and perennial nitrcline overlap (e.g. Canada Basin)



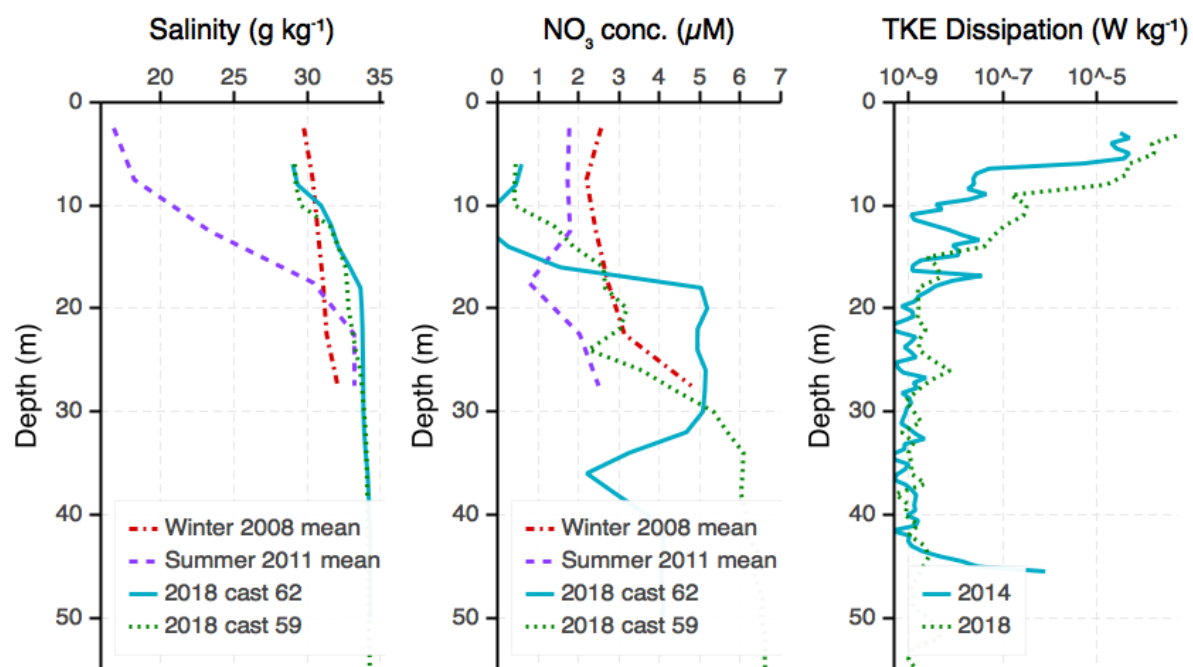
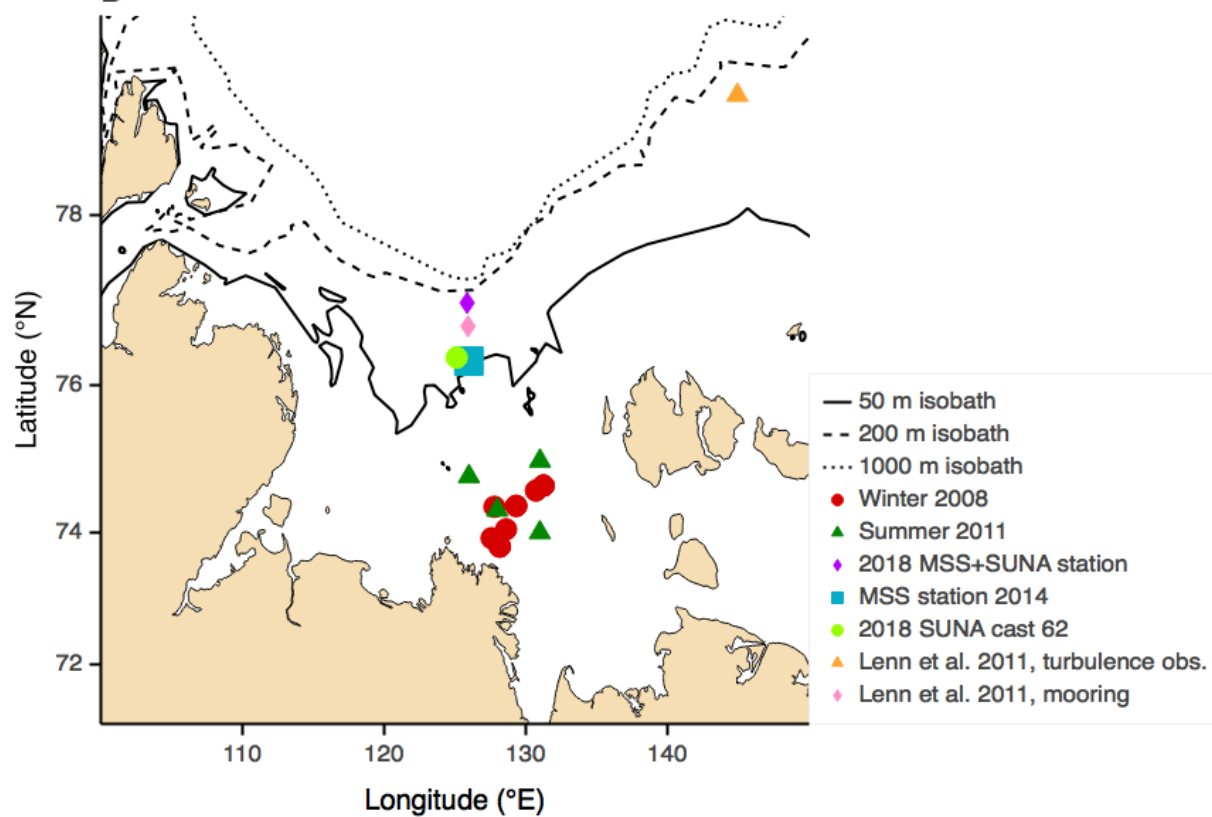
724

725 *Figure 9: A simplified marine nitrogen cycle and idealized Arctic hydrography. (A) General*
 726 *schematic of a vertical profile of nitrate concentration, along with the respective portion of*
 727 *the nitrogen cycle that takes place in each layer. In this idealized case, there is a clear*
 728 *separation between the seasonal variations in nitrate concentrations in the surface layer*
 729 *which give rise to the seasonal nitrcline, and the underlying perennial nitrcline. (B) In areas*
 730 *with deep overturning into the waters of maximum nitrate concentration, the deep nitrcline*
 731 *ceases to be meaningful. Instead, nitrate fluxes tap into high-nutrient water every winter. (C)*

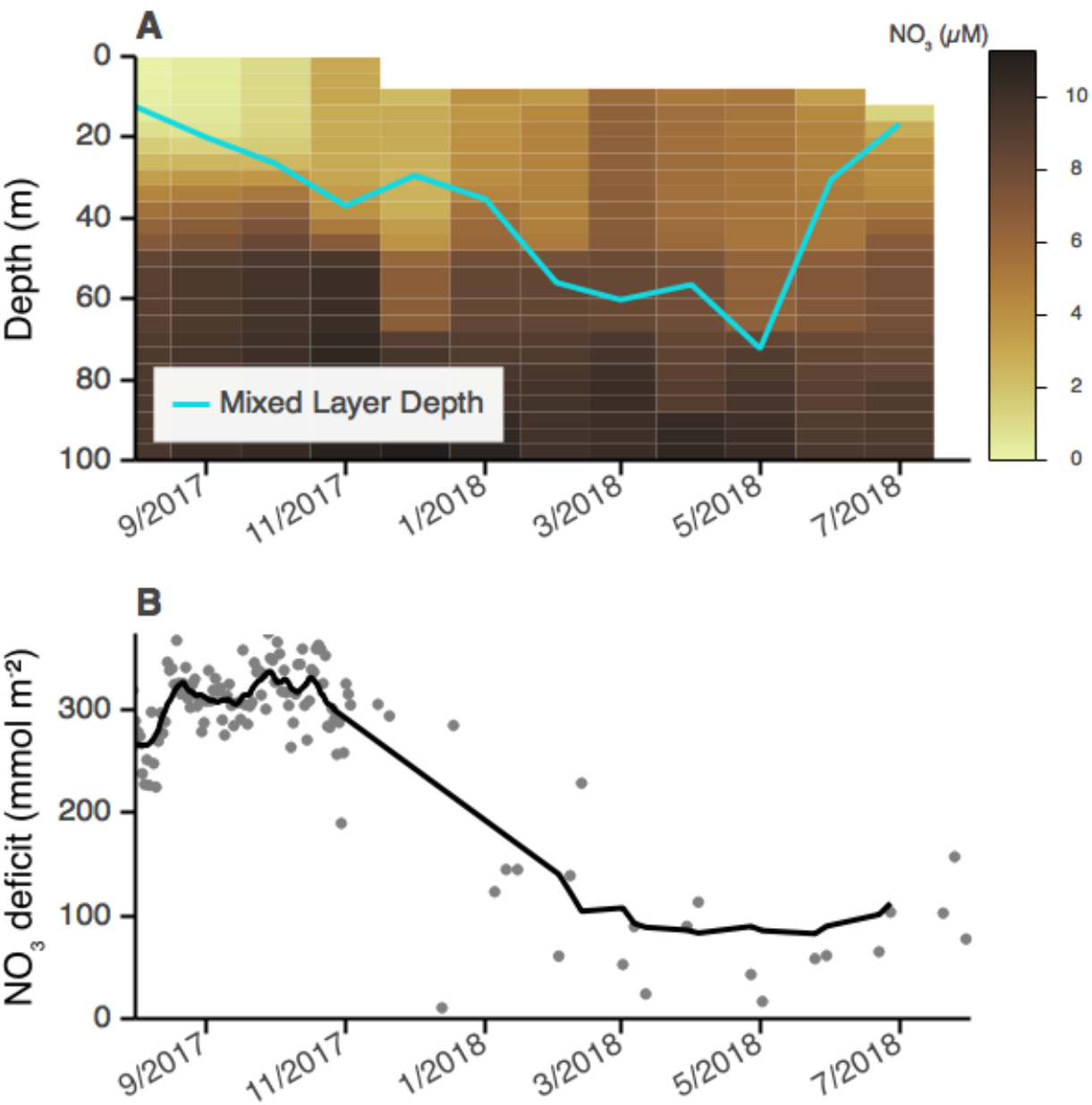
732 *Highly stratified areas do not see large seasonal excursions in surface layer nitrate*
733 *concentrations or mixing depths.*



735 *Figure 10: Young Sound data. (A) Bathymetry and coast data courtesy T. Vang and J.*
736 *Bendtsen (Rysgaard et al. (2003); not included in the supplemental material). Transect*
737 *starting in the inner end of the fjord, going over two sills and out into the Greenland Sea,*
738 *demonstrating (B) low salinity due to ice sheet runoff, (C) nitrate depletion in the upper 30-40*
739 *meters, and (D) a quiescent fjord interior with vigorous mixing over the two sills. (E) Upward*
740 *nitrate fluxes observed in Young Sound (shaded areas represent kernel density estimates) and*
741 *observed values of new production, integrated over 0-20 meters (black bars). Note that new*
742 *production estimates are based on only two measurement depths; see methods.*

A**B**

744 Figure 11: Laptev Sea data. (A) Vertical profiles of salinity, nitrate concentration and
 745 dissipation of turbulent kinetic energy (ϵ) in the Laptev Sea. (B) Measurement locations in the
 746 Laptev Sea.



747
 748 Figure 12: Seasonal cycle of nitrate concentrations in Baffin Bay alongside mixed layer depth
 749 (A) and the 0-60 m vertically integrated nitrate deficit $\Delta[\text{NO}_3^-] = [\text{NO}_3^-](60\text{m}) - [\text{NO}_3^-](z)$
 750 (B).

751 14 Tables

752 Table 1: Nitrate fluxes observed in the Arctic Ocean. * Turbulent vertical nitrate flux given in
 753 $\text{mmol N m}^{-2} \text{d}^{-1}$. ** Under ice cover. *** Open water. AABC: Anticyclonic Arctic Boundary

754 *Current. Perennial: Measured below the extent of seasonal nitrate variation. See*
 755 *Supplementary Material for complete data set.*

Region	Season	NO ₃ ⁻ flux*	Reference	Sample size	Turbulence meas.	NO ₃ ⁻ meas.
Amundsen Basin	Winter	0.05	Randelhoff and Guthrie (2016)	Large	Microstruct.	Optic
Baffin Bay	Winter	1.7	this study	Large	N/A	Optic
Barents Sea	Summer	0.1	Sundfjord et al. (2007)	Small	Microstruct.	Bottle
Barents Sea	Summer	0.1	Wiedmann et al. (2017)	Small	Microstruct.	Optic
Barents Sea	Summer	2.0	Sundfjord et al. (2007)	Small	Microstruct.	Bottle
Barents Sea	Summer	5.0	Wiedmann et al. (2017)	Small	Microstruct.	Optic
Barents Sea, AABC	Winter	2.5	Randelhoff et al. (2015)	Large	N/A	Optic
Beaufort Sea	Winter	0.12	Bourgault et al. (2011)	Large	Microstruct.	Optic
Canada Basin	Winter	0.01	Randelhoff and Guthrie (2016)	Large	Finestruct.	Optic
Chukchi Sea	Summer	0.02	this study, Nishino et al. (2015)	Small	Microstruct.	Bottle
Chukchi Sea	Summer	0.19	Nishino et al. (2018)	Large	Microstruct.	Bottle
Laptev Shelf (outer)	Summer	0.015	this study	Small	Microstruct.	Bottle & Optic
Makarov Basin	Winter	0.015	Randelhoff and Guthrie (2016)	Large	Finestruct.	Optic
N Svalbard/Fram Strait	Summer	0.3**	Randelhoff et al. (2016)	Large	Microstruct.	Optic
N Svalbard/Fram Strait	Summer	0.7***	Randelhoff et al. (2016)	Large	Microstruct.	Optic
Nansen Basin/Yermak Plateau	Winter	0.2	Randelhoff and Guthrie (2016)	Large	Microstruct.	Optic
Young Sound (Interior)	Summer	0.035	this study	Large	Microstruct.	Optic
Young Sound (Sills)	Summer	0.33	this study	Large	Microstruct.	Optic

756
757
758

759 *Table 2: Nitrate fluxes in the global ocean, excluding the Arctic. * Turbulent vertical nitrate*
760 *flux given in mmol N m⁻² d⁻¹.*

Reference	NO ₃ ⁻ flux*	Region
Lewis et al. (1986)	0.14	Subtropical North Atlantic
Jenkins (1988)	1.6	Subtropical North Atlantic
Hamilton et al. (1989) re-analyzing Lewis et al. (1986)	0.85	Subtropical North Atlantic
Carr et al. (1995)	1.9	Equatorial Pacific (5 °N - 5 °S)
Carr et al. (1995)	4.3	Equatorial Pacific (1 °N - 1 °S)
Horne et al. (1996)	0.047	North Atlantic, Georges Bank
Horne et al. (1996)	0.18	North Atlantic, Georges Bank
Planas et al. (1999)	0.38	Central Atlantic
Law et al. (2001)	1.8	Subarctic North Atlantic
Sharples et al. (2001)	12.0	New Zealand Shelf
Law (2003)	0.17	Antarctic Circumpolar Current
Hales (2005)	9.0	Oregon Shelf Upwelling System
Sharples et al. (2007)	1.3	Celtic Sea shelf edge (neap tide)
Sharples et al. (2007)	9.0	Celtic Sea shelf edge (spring tide)
Hales et al. (2009)	0.9	New England shelf break front (seaward side)
Hales et al. (2009)	5.2	New England shelf break front (shoreward side)
Rippeth et al. (2009)	1.5	Irish Sea
Martin et al. (2010)	0.09	North Atlantic, Porcupine Abyssal Plain
Schafstall et al. (2010)	1.0	Mauritanian Upwelling (offshore)
Schafstall et al. (2010)	3.7	Mauritanian Upwelling (shelf)
Schafstall et al. (2010)	10.0	Mauritanian Upwelling (slope)
Shiozaki et al. (2011)	0.25	North Pacific, East China Sea shelf
Kaneko et al. (2013)	0.003	North Pacific, Kuroshio (south of front)
Kaneko et al. (2013)	0.34	North Pacific, Kuroshio (north of front)
Cyr et al. (2015)	0.21	St. Lawrence Gulf, Canada

15 References

- Aagaard, K., and Carmack, E. C. (1989). The role of sea ice and other fresh water in the Arctic circulation. *Journal of Geophysical Research: Oceans* 94, 14485–14498. doi:[10.1029/JC094iC10p14485](https://doi.org/10.1029/JC094iC10p14485).
- Agawin, N. S. R., Duarte, C. M., and Agustí, S. (2000). Nutrient and temperature control of the contribution of picoplankton to phytoplankton biomass and production. *Limnology and Oceanography* 45, 591–600. doi:[10.4319/lo.2000.45.3.0591](https://doi.org/10.4319/lo.2000.45.3.0591).
- Alkire, M. (2019). Ocean conductivity, temperature, density (CTD), oxygen, and nitrate profiles, Eurasian and Makarov basins, Arctic Ocean, 2013-2018. doi:[10.18739/A24X54G9W](https://doi.org/10.18739/A24X54G9W).
- Alkire, M. B., Falkner, K. K., Morison, J., Collier, R. W., Guay, C. K., Desiderio, R. A., et al. (2010). Sensor-based profiles of the NO parameter in the central Arctic and southern Canada Basin New insights regarding the cold halocline. *Deep-Sea Research Part I- Oceanographic Research Papers* 57, 1432–1443. doi:[10.1016/j.dsr.2010.07.011](https://doi.org/10.1016/j.dsr.2010.07.011).
- Allen, T. F. H., and Hoekstra, T. W. (2015). *Toward a unified ecology*. Second edition. New York: Columbia University Press.
- Ambühl, H. (1959). Die Bedeutung der Strömung als ökologischer Faktor. *Schweizerische Zeitschrift für Hydrologie* 21, 133. doi:[10.1007/BF02505455](https://doi.org/10.1007/BF02505455).
- Ardyna, M., Babin, M., Gosselin, M., Devred, E., Rainville, L., and Tremblay, J.-É. (2014). Recent Arctic Ocean sea ice loss triggers novel fall phytoplankton blooms. *Geophysical Research Letters* 41, 6207–6212. doi:[10.1002/2014gl061047](https://doi.org/10.1002/2014gl061047).
- Arrigo, K. R., Mills, M. M., Dijken, G. L. van, Lowry, K. E., Pickart, R. S., and Schlitzer, R. (2017). Late Spring Nitrate Distributions Beneath the Ice-Covered Northeastern Chukchi Shelf. *Journal of Geophysical Research: Biogeosciences* 122, 2409–2417. doi:[10.1002/2017JG003881](https://doi.org/10.1002/2017JG003881).
- Bauch, D., Cherniavskaia, E., Novikhin, A., and Kassens, H. (2018). Physical oceanography, nutrients, and $\Delta^{18}\text{O}$ measured on water bottle samples in the Laptev Sea, supplement to: Bauch, D; Cherniavskaia, Ekaterina (2018): Water Mass Classification on a Highly Variable Arctic Shelf Region: Origin of Laptev Sea Water Masses and Implications for the Nutrient Budget. *Journal of Geophysical Research: Oceans*. doi:[10.1594/PANGAEA.885448](https://doi.org/10.1594/PANGAEA.885448).
- Biogeochemical-Argo Planning Group (2016). The scientific rationale, design and implementation plan for a Biogeochemical-Argo float array. Ifremer doi:[10.13155/46601](https://doi.org/10.13155/46601).
- Blais, M., Tremblay, J.-É., Jungblut, A. D., Gagnon, J., Martin, J., Thaler, M., et al. (2012). Nitrogen fixation and identification of potential diazotrophs in the Canadian Arctic. *Global Biogeochemical Cycles* 26. doi:[10.1029/2011gb004096](https://doi.org/10.1029/2011gb004096).

796 Bluhm, B. A., Kosobokova, K. N., and Carmack, E. C. (2015). A tale of two basins: An
797 integrated physical and biological perspective of the deep Arctic Ocean. *Progress in*
798 *Oceanography* 139, 89–121. doi:[10.1016/j.pocean.2015.07.011](https://doi.org/10.1016/j.pocean.2015.07.011).

799 Bokeh Development Team (2018). *Bokeh: Python library for interactive visualization*.

800 Bouffard, D., and Boegman, L. (2013). A diapycnal diffusivity model for stratified
801 environmental flows. *Dynamics of Atmospheres and Oceans* 61-62, 14–34.
802 doi:[10.1016/j.dynatmoce.2013.02.002](https://doi.org/10.1016/j.dynatmoce.2013.02.002).

803 Bouman, H. A., Platt, T., Doblin, M., Figueiras, F. G., Gudmundsson, K., Gudfinnsson, H. G., et
804 al. (2018). Photosynthesis-Irradiance parameters of marine phytoplankton: Synthesis of a
805 global data set. *Earth System Science Data* 10, 251–266. doi:[https://doi.org/10.5194/essd-](https://doi.org/10.5194/essd-10-251-2018)
806 [10-251-2018](https://doi.org/10.5194/essd-10-251-2018).

807 Bourgault, D., Hamel, C., Cyr, F., Tremblay, J.-É., Galbraith, P. S., Dumont, D., et al. (2011).
808 Turbulent nitrate fluxes in the Amundsen Gulf during ice-covered conditions. *Geophysical*
809 *Research Letters* 38. doi:[10.1029/2011GL047936](https://doi.org/10.1029/2011GL047936).

810 Brzezinski, M. A. (1985). The Si:C:N ratio of marine diatoms: Interspecific variability and
811 the effect of some environmental variables. *Journal of Phycology* 21, 347–357.

812 Cai, P., Rutgers van der Loeff, M., Stimac, I., Năthig, E.-M., Lepore, K., and Moran, S. B.
813 (2010). Low export flux of particulate organic carbon in the central Arctic Ocean as
814 revealed by ²³⁴Th:²³⁸U disequilibrium. *Journal of Geophysical Research: Oceans* 115, n/a–
815 n/a. doi:[10.1029/2009JC005595](https://doi.org/10.1029/2009JC005595).

816 Carmack, E., Barber, D., Christensen, J., Macdonald, R., Rudels, B., and Sakshaug, E. (2006).
817 Climate variability and physical forcing of the food webs and the carbon budget on
818 panarctic shelves. *Progress in Oceanography* 71, 145–181.
819 doi:[10.1016/j.pocean.2006.10.005](https://doi.org/10.1016/j.pocean.2006.10.005).

820 Carmack, E. C. (2007). The alpha/beta ocean distinction: A perspective on freshwater
821 fluxes, convection, nutrients and productivity in high-latitude seas. *Deep Sea Research Part*
822 *II: Topical Studies in Oceanography* 54, 2578–2598. doi:[10.1016/j.dsr2.2007.08.018](https://doi.org/10.1016/j.dsr2.2007.08.018).

823 Carmack, E., and Chapman, D. C. (2003). Wind-driven shelf/basin exchange on an Arctic
824 shelf: The joint roles of ice cover extent and shelf-break bathymetry. *Geophys. Res. Lett.* 30.
825 doi:[10.1029/2003gl017526](https://doi.org/10.1029/2003gl017526).

826 Carmack, E., and Wassmann, P. (2006). Food webs and physical - biological coupling on
827 pan-Arctic shelves: Unifying concepts and comprehensive perspectives. *Progress in*
828 *Oceanography* 71, 446–477. doi:[10.1016/j.pocean.2006.10.004](https://doi.org/10.1016/j.pocean.2006.10.004).

829 Carr, M.-E., Lewis, M. R., Kelley, D., and Jones, B. (1995). A physical estimate of new
830 production in the equatorial Pacific along 150W. *Limnology and Oceanography* 40, 138–
831 147. doi:[10.4319/lo.1995.40.1.0138](https://doi.org/10.4319/lo.1995.40.1.0138).

832 Chanona, M., Waterman, S., and Gratton, Y. (2018). Variability of Internal Wave-Driven
833 Mixing and Stratification in Canadian Arctic Shelf and Shelf-Slope Waters. *Journal of*
834 *Geophysical Research: Oceans* 123, 9178–9195. doi:[10.1029/2018JC014342](https://doi.org/10.1029/2018JC014342).

835 Chisholm, S. W. (1992). “Phytoplankton Size,” in *Primary Productivity and Biogeochemical*
836 *Cycles in the Sea* Environmental Science Research., eds. P. G. Falkowski, A. D. Woodhead,
837 and K. Vivirito (Boston, MA: Springer US), 213–237. doi:[10.1007/978-1-4899-0762-2_12](https://doi.org/10.1007/978-1-4899-0762-2_12).

838 Cochlan, W. P., and Harrison, P. J. (1991). Kinetics of nitrogen (nitrate, ammonium and
839 urea) uptake by the picoflagellate *Micromonas pusilla* (Prasinophyceae). *Journal of*
840 *Experimental Marine Biology and Ecology* 153, 129–141. doi:[10.1016/0022-](https://doi.org/10.1016/0022-0981(91)90220-Q)
841 [0981\(91\)90220-Q](https://doi.org/10.1016/0022-0981(91)90220-Q).

842 Codispoti, L. A., Kelly, V., Thessen, A., Matrai, P., Suttles, S., Hill, V., et al. (2013). Synthesis of
843 primary production in the Arctic Ocean: III. Nitrate and phosphate based estimates of net
844 community production. *Progress in Oceanography* 110, 126–150.
845 doi:[10.1016/j.pocean.2012.11.006](https://doi.org/10.1016/j.pocean.2012.11.006).

846 Cole, S. T., Toole, J. M., Rainville, L., and Lee, C. M. (2018). Internal waves in the Arctic:
847 Influence of ice concentration, ice roughness, and surface layer stratification. *Journal of*
848 *Geophysical Research: Oceans*. doi:[10.1029/2018JC014096](https://doi.org/10.1029/2018JC014096).

849 Comiso, J. C. (2012). Large decadal decline of the Arctic multiyear ice cover. *Journal of*
850 *Climate* 25, 1176–1193. doi:[10.1175/JCLI-D-11-00113.1](https://doi.org/10.1175/JCLI-D-11-00113.1).

851 Crews, L., Sundfjord, A., Albretsen, J., and Hattermann, T. (2018). Mesoscale Eddy Activity
852 and Transport in the Atlantic Water Inflow Region North of Svalbard. *Journal of Geophysical*
853 *Research: Oceans* 123, 201–215. doi:[10.1002/2017JC013198](https://doi.org/10.1002/2017JC013198).

854 Cyr, F., Bourgault, D., Galbraith, P. S., and Gosselin, M. (2015). Turbulent nitrate fluxes in the
855 Lower St. Lawrence Estuary (Canada). *J. Geophys. Res. Oceans*, n/a–n/a.
856 doi:[10.1002/2014jc010272](https://doi.org/10.1002/2014jc010272).

857 Dosser, H. V., and Rainville, L. (2016). Dynamics of the Changing Near-Inertial Internal
858 Wave Field in the Arctic Ocean. *Journal of Physical Oceanography* 46, 395–415.
859 doi:[10.1175/jpo-d-15-0056.1](https://doi.org/10.1175/jpo-d-15-0056.1).

860 Dugdale, R. C., and Goering, J. J. (1967). Uptake of new and regenerated forms of nitrogen in
861 primary productivity. *Limnology and Oceanography* 12, 196–206.
862 doi:[10.4319/lo.1967.12.2.0196](https://doi.org/10.4319/lo.1967.12.2.0196).

863 Eppley, R. W., Rogers, J. N., and McCarthy, J. J. (1969). Half-Saturation Constants for Uptake
864 of Nitrate and Ammonium by Marine Phytoplankton1. *Limnology and Oceanography* 14,
865 912–920. doi:[10.4319/lo.1969.14.6.0912](https://doi.org/10.4319/lo.1969.14.6.0912).

866 Fer, I., and Drinkwater, K. (2014). Mixing in the Barents Sea Polar Front near Hopen in
867 spring. *Journal of Marine Systems* 130, 206–218. doi:[10.1016/j.jmarsys.2012.01.005](https://doi.org/10.1016/j.jmarsys.2012.01.005).

868 Frey, K. E., and McClelland, J. W. (2009). Impacts of permafrost degradation on arctic river
869 biogeochemistry. *Hydrological Processes* 23, 169–182. doi:[10.1002/hyp.7196](https://doi.org/10.1002/hyp.7196).

870 Frigstad, H., Andersen, T., Bellerby, R. G. J., Silyakova, A., and Hessen, D. O. (2014). Variation
871 in the seston C:N ratio of the Arctic Ocean and pan-Arctic shelves. *Journal of Marine Systems*
872 129, 214–223. doi:[10.1016/j.jmarsys.2013.06.004](https://doi.org/10.1016/j.jmarsys.2013.06.004).

873 Gargett, A., and Garner, T. (2008). Determining Thorpe Scales from Ship-Lowered CTD
874 Density Profiles. *Journal of Atmospheric and Oceanic Technology* 25, 1657–1670.
875 doi:[10.1175/2008jtecho541.1](https://doi.org/10.1175/2008jtecho541.1).

876 Garrett, C., and Munk, W. (1975). Space-time scales of internal waves: A progress report.
877 *Journal of Geophysical Research* 80, 291–297. doi:[10.1029/JC080i003p00291](https://doi.org/10.1029/JC080i003p00291).

878 Gregg, M. C., D’Asaro, E. A., Riley, J. J., and Kunze, E. (2018). Mixing Efficiency in the Ocean.
879 *Annual Review of Marine Science* 10, 443–473. doi:[10.1146/annurev-marine-121916-](https://doi.org/10.1146/annurev-marine-121916-063643)
880 [063643](https://doi.org/10.1146/annurev-marine-121916-063643).

881 Guthrie, J. D., Morison, J. H., and Fer, I. (2013). Revisiting internal waves and mixing in the
882 Arctic Ocean. *Journal of Geophysical Research: Oceans* 118, 3966–3977.
883 doi:[10.1002/jgrc.20294](https://doi.org/10.1002/jgrc.20294).

884 Hales, B. (2005). Irreversible nitrate fluxes due to turbulent mixing in a coastal upwelling
885 system. *Journal of Geophysical Research* 110, C10S11. doi:[10.1029/2004JC002685](https://doi.org/10.1029/2004JC002685).

886 Hales, B., Hebert, D., and Marra, J. (2009). Turbulent supply of nutrients to phytoplankton
887 at the New England shelf break front. *Journal of Geophysical Research* 114, C05010.
888 doi:[10.1029/2008JC005011](https://doi.org/10.1029/2008JC005011).

889 Hamilton, J. M., Lewis, M. R., and Ruddick, B. R. (1989). Vertical fluxes of nitrate associated
890 with salt fingers in the world’s oceans. *Journal of Geophysical Research: Oceans* 94, 2137–
891 2145. doi:[10.1029/JC094iC02p02137](https://doi.org/10.1029/JC094iC02p02137).

892 Hattermann, T., Isachsen, P. E., von Appen, W.-J., Albretsen, J., and Sundfjord, A. (2016).
893 Eddy-driven recirculation of Atlantic Water in Fram Strait. *Geophysical Research Letters* 43,
894 3406–3414. doi:[10.1002/2016gl068323](https://doi.org/10.1002/2016gl068323).

895 Holding, J. M., Markager, S., Juul-Pedersen, T., Paulsen, M. L., Møller, E. F., Meire, L., et al.
896 (2019). Seasonal and spatial patterns of primary production in a high-latitude fjord
897 affected by Greenland Ice Sheet run-off. *Biogeosciences* 16, 3777–3792.
898 doi:<https://doi.org/10.5194/bg-16-3777-2019>.

899 Honjo, S., Krishfield, R. A., Eglinton, T. I., Manganini, S. J., Kemp, J. N., Doherty, K., et al.
900 (2010). Biological pump processes in the cryopelagic and hemipelagic Arctic Ocean: Canada
901 Basin and Chukchi Rise. *Progress in Oceanography* 55, 137–170.
902 doi:<http://dx.doi.org/10.1016/j.pocean.2010.02.009>.

903 Hopwood, M. J., Carroll, D., Browning, T., Meire, L., Mortensen, J., Krisch, S., et al. (2018).
 904 Non-linear response of summertime marine productivity to increased meltwater discharge
 905 around Greenland. *Nature communications* 9, 3256.

906 Hopwood, M. J., Carroll, D., Dunse, T., Hodson, A., Holding, J. M., Iriarte, J. L., et al. (2019).
 907 How does glacier discharge affect marine biogeochemistry and primary production in the
 908 Arctic? *The Cryosphere Discussions*, 1–51.

909 Horne, E. P. W., Loder, J. W., Naime, C. E., and Oakey, N. S. (1996). Turbulence dissipation
 910 rates and nitrate supply in the upper water column on Georges Bank. *Deep Sea Research*
 911 *Part II: Topical Studies in Oceanography* 43, 1683–1712. doi:[10.1016/S0967-](https://doi.org/10.1016/S0967-0645(96)00037-9)
 912 [0645\(96\)00037-9](https://doi.org/10.1016/S0967-0645(96)00037-9).

913 Ivanov, V., Alexeev, V., Koldunov, N. V., Repina, I., Sandø, A. B., Smedsrud, L. H., et al. (2016).
 914 Arctic Ocean heat impact on regional ice decay - a suggested positive feedback. *Journal of*
 915 *Physical Oceanography* 46, 1437–1456. doi:[10.1175/jpo-d-15-0144.1](https://doi.org/10.1175/jpo-d-15-0144.1).

916 Jenkins, W. J. (1988). Nitrate flux into the euphotic zone near Bermuda. *Nature* 331, 521–
 917 523. doi:[10.1038/331521a0](https://doi.org/10.1038/331521a0).

918 Johnson, K. S., Riser, S. C., and Karl, D. M. (2010). Nitrate supply from deep to near-surface
 919 waters of the North Pacific subtropical gyre. *Nature* 465, 1062–1065.
 920 doi:[10.1038/nature09170](https://doi.org/10.1038/nature09170).

921 Kalvelage, T., Jensen, M. M., Contreras, S., Revsbech, N. P., Lam, P., Günter, M., et al. (2011).
 922 Oxygen sensitivity of anammox and coupled N-cycle processes in oxygen minimum zones.
 923 *PloS one* 6, e29299.

924 Kaneko, H., Yasuda, I., Komatsu, K., and Itoh, S. (2013). Observations of vertical turbulent
 925 nitrate flux across the Kuroshio. *Geophysical Research Letters* 40, 3123–3127.
 926 doi:[10.1002/grl.50613](https://doi.org/10.1002/grl.50613).

927 Karp-Boss, L., Boss, E. S., and Jumars, P. A. (1996). Nutrient fluxes to planktonic osmotrophs
 928 in the presence of fluid motion. *Oceanography and Marine Biology: an Annual Review* 34,
 929 71–107.

930 Kämpf, J., and Chapman, P. (2016). *Upwelling Systems of the World*. Springer.

931 Kiørboe, T. (2008). *A mechanistic approach to plankton ecology*. Princeton: Princeton
 932 University Press.

933 Kowalik, Z., and Proshutinsky, A. Y. (2013). “The Arctic Ocean Tides,” in *The Polar Oceans*
 934 *and Their Role in Shaping the Global Environment* (American Geophysical Union (AGU)),
 935 137–158. doi:[10.1029/GM085p0137](https://doi.org/10.1029/GM085p0137).

936 Law, C. S. (2003). Vertical eddy diffusion and nutrient supply to the surface mixed layer of
 937 the Antarctic Circumpolar Current. *Journal of Geophysical Research* 108, 3272.
 938 doi:[10.1029/2002JC001604](https://doi.org/10.1029/2002JC001604).

939 Law, C. S., Martin, A. P., Liddicoat, M. I., Watson, A. J., Richards, K. J., and Woodward, E. M. S.
 940 (2001). A Lagrangian SF6 tracer study of an anticyclonic eddy in the North Atlantic: Patch
 941 evolution, vertical mixing and nutrient supply to the mixed layer. *Deep Sea Research Part II:
 942 Topical Studies in Oceanography* 48, 705–724. doi:[10.1016/S0967-0645\(00\)00112-0](https://doi.org/10.1016/S0967-0645(00)00112-0).

943 Lewis, M. R., Hebert, D., Harrison, W. G., Platt, T., and Oakey, N. S. (1986). Vertical Nitrate
 944 Fluxes in the Oligotrophic Ocean. *Science* 234, 870–873. doi:[10.1126/science.234.4778.870](https://doi.org/10.1126/science.234.4778.870).

945 Lincoln, B. J., Rippeth, T. P., Lenn, Y.-D., Timmermans, M. L., Williams, W. J., and Bacon, S.
 946 (2016). Wind-driven mixing at intermediate depths in an ice-free Arctic Ocean. *Geophysical
 947 Research Letters* 43, 9749–9756. doi:[10.1002/2016GL070454](https://doi.org/10.1002/2016GL070454).

948 Loeng, H. (1991). Features of the physical oceanographic conditions of the Barents Sea.
 949 *Polar Research* 10, 5–18. doi:[10.1111/j.1751-8369.1991.tb00630.x](https://doi.org/10.1111/j.1751-8369.1991.tb00630.x).

950 Lueck, R. G., Wolk, F., and Yamazaki, H. (2002). Oceanic Velocity Microstructure
 951 Measurements in the 20th Century. *Journal of Oceanography* 58, 153–174.
 952 doi:[10.1023/A:1015837020019](https://doi.org/10.1023/A:1015837020019).

953 Margalef, R. (1978). Life-forms of phytoplankton as survival alternatives in an unstable
 954 environment. *Oceanologica acta* 1, 493–509.

955 Martin, A. P., Lucas, M. I., Painter, S. C., Pidcock, R., Prandke, H., Prandke, H., et al. (2010).
 956 The supply of nutrients due to vertical turbulent mixing: A study at the Porcupine Abyssal
 957 Plain study site in the northeast Atlantic. *Deep Sea Research Part II: Topical Studies in
 958 Oceanography* 57, 1293–1302. doi:[10.1016/j.dsr2.2010.01.006](https://doi.org/10.1016/j.dsr2.2010.01.006).

959 Martin, A. P., and Pondaven, P. (2003). On estimates for the vertical nitrate flux due to eddy
 960 pumping. *Journal of Geophysical Research: Oceans* 108, n/a–n/a.
 961 doi:[10.1029/2003JC001841](https://doi.org/10.1029/2003JC001841).

962 Martin, A. P., and Richards, K. J. (2001). Mechanisms for vertical nutrient transport within a
 963 North Atlantic mesoscale eddy. *Deep Sea Research Part II: Topical Studies in Oceanography*
 964 48, 757–773. doi:[10.1016/S0967-0645\(00\)00096-5](https://doi.org/10.1016/S0967-0645(00)00096-5).

965 Martin, T., Tsamados, M., Schroeder, D., and Feltham, D. L. (2016). The impact of variable
 966 sea ice roughness on changes in Arctic Ocean surface stress: A model study. *Journal of
 967 Geophysical Research: Oceans* 121, 1931–1952. doi:[10.1002/2015JC011186](https://doi.org/10.1002/2015JC011186).

968 McPhee, M. G., and Kantha, L. H. (1989). Generation of internal waves by sea ice. *Journal of
 969 Geophysical Research: Oceans* 94, 3287–3302. doi:[10.1029/JC094iC03p03287](https://doi.org/10.1029/JC094iC03p03287).

970 McPhee, M. G., and Stanton, T. P. (1996). Turbulence in the statically unstable oceanic
 971 boundary layer under Arctic leads. *Journal of Geophysical Research: Oceans* 101, 6409–
 972 6428. doi:[10.1029/95JC03842](https://doi.org/10.1029/95JC03842).

973 Meier, W. N., Hovelsrud, G. K., van Oort, B. E. H., Key, J. R., Kovacs, K. M., Michel, C., et al.
 974 (2014). Arctic sea ice in transformation: A review of recent observed changes and impacts

975 on biology and human activity: ARCTIC SEA ICE: REVIEW OF RECENT CHANGES. *Reviews of*
 976 *Geophysics* 52, 185–217. doi:[10.1002/2013RG000431](https://doi.org/10.1002/2013RG000431).

977 Meire, L., Meire, P., Struyf, E., Krawczyk, D. W., Arendt, K. E., Yde, J. C., et al. (2016). High
 978 export of dissolved silica from the Greenland Ice Sheet: Silica Export the Ice Sheet.
 979 *Geophysical Research Letters* 43, 9173–9182. doi:[10.1002/2016GL070191](https://doi.org/10.1002/2016GL070191).

980 Meire, L., Mortensen, J., Meire, P., Juul-Pedersen, T., Sejr, M. K., Rysgaard, S., et al. (2017).
 981 Marine-terminating glaciers sustain high productivity in Greenland fjords. *Global Change*
 982 *Biology* 23, 5344–5357. doi:[10.1111/gcb.13801](https://doi.org/10.1111/gcb.13801).

983 Moore, C. M., Mills, M. M., Arrigo, K. R., Berman-Frank, I., Bopp, L., Boyd, P. W., et al. (2013).
 984 Processes and patterns of oceanic nutrient limitation. *Nature Geoscience* 6, 701–710.
 985 doi:[10.1038/ngeo1765](https://doi.org/10.1038/ngeo1765).

986 Moran, S. B., Weinstein, S. E., Edmonds, H. N., Smith, J. N., Kelly, R. P., Pilson, M. E. Q., et al.
 987 (2003). Does $^{234}\text{Th}/^{238}\text{U}$ disequilibrium provide an accurate record of the export flux of
 988 particulate organic carbon from the upper ocean? *Limnology and Oceanography* 48, 1018–
 989 1029. doi:[10.4319/lo.2003.48.3.1018](https://doi.org/10.4319/lo.2003.48.3.1018).

990 Moum, J. N., Gregg, M. C., Lien, R. C., and Carr, M. E. (1995). Comparison of Turbulence
 991 Kinetic Energy Dissipation Rate Estimates from Two Ocean Microstructure Profilers.
 992 *Journal of Atmospheric and Oceanic Technology* 12, 346–366. doi:[10.1175/1520-0426\(1995\)012<0346:COTKED>2.0.CO;2](https://doi.org/10.1175/1520-0426(1995)012<0346:COTKED>2.0.CO;2).

994 Nishino, S., Kawaguchi, Y., Fujiwara, A., Shiozaki, T., Aoyama, M., Harada, N., et al. (2018).
 995 Biogeochemical Anatomy of a Cyclonic Warm-Core Eddy in the Arctic Ocean. *Geophysical*
 996 *Research Letters* 45. doi:[10.1029/2018GL079659](https://doi.org/10.1029/2018GL079659).

997 Nishino, S., Kawaguchi, Y., Inoue, J., Hirawake, T., Fujiwara, A., Futsuki, R., et al. (2015).
 998 Nutrient supply and biological response to wind-induced mixing, inertial motion, internal
 999 waves, and currents in the northern Chukchi Sea. *Journal of Geophysical Research: Oceans*
 1000 120, 1975–1992. doi:[10.1002/2014jc010407](https://doi.org/10.1002/2014jc010407).

1001 Nummelin, A., Ilicak, M., Li, C., and Smedsrud, L. H. (2015). Consequences of future
 1002 increased Arctic runoff on Arctic Ocean stratification, circulation, and sea ice cover. *Journal*
 1003 *of Geophysical Research: Oceans*. doi:[10.1002/2015jc011156](https://doi.org/10.1002/2015jc011156).

1004 Omand, M. M., Feddersen, F., Guza, R. T., and Franks, P. J. S. (2012). Episodic vertical
 1005 nutrient fluxes and nearshore phytoplankton blooms in Southern California. *Limnology and*
 1006 *Oceanography* 57, 1673–1688. doi:[10.4319/lo.2012.57.6.1673](https://doi.org/10.4319/lo.2012.57.6.1673).

1007 Onarheim, I. H., Eldevik, T., Smedsrud, L. H., and Stroeve, J. C. (2018). Seasonal and Regional
 1008 Manifestation of Arctic Sea Ice Loss. *Journal of Climate* 31, 4917–4932. doi:[10.1175/JCLI-D-17-0427.1](https://doi.org/10.1175/JCLI-D-17-0427.1).

1010 Osborn, T. R. (1980). Estimates of the Local Rate of Vertical Diffusion from Dissipation
 1011 Measurements. *J. Phys. Oceanogr.* 10, 83–89. doi:[10.1175/1520-0485\(1980\)010<0083:EOTLRO>2.0.CO;2](https://doi.org/10.1175/1520-0485(1980)010<0083:EOTLRO>2.0.CO;2).

- 1013 Padman, L. (1995). "Small-scale physical processes in the Arctic Ocean," in *Coastal and*
1014 *Estuarine Studies*, eds. W. O. Smith and J. M. Grebmeier (Washington, D. C.: American
1015 Geophysical Union), 97–129. doi:[10.1029/CE049p0097](https://doi.org/10.1029/CE049p0097).
- 1016 Paulsen, M. L., Nielsen, S. E. B., Müller, O., Møller, E. F., Stedmon, C. A., Juul-Pedersen, T., et
1017 al. (2017). Carbon Bioavailability in a High Arctic Fjord Influenced by Glacial Meltwater, NE
1018 Greenland. *Frontiers in Marine Science* 4. doi:[10.3389/fmars.2017.00176](https://doi.org/10.3389/fmars.2017.00176).
- 1019 Paulsen, M. L., Seuthe, L., Reigstad, M., Larsen, A., Cape, M. R., and Vernet, M. (2018).
1020 Asynchronous Accumulation of Organic Carbon and Nitrogen in the Atlantic Gateway to the
1021 Arctic Ocean. *Frontiers in Marine Science* 5. doi:[10.3389/fmars.2018.00416](https://doi.org/10.3389/fmars.2018.00416).
- 1022 Peralta-Ferriz, C., and Woodgate, R. A. (2015). Seasonal and interannual variability of pan-
1023 Arctic surface mixed layer properties from 1979 to 2012 from hydrographic data, and the
1024 dominance of stratification for multiyear mixed layer depth shoaling. *Progress in*
1025 *Oceanography* 134, 19–53. doi:<http://dx.doi.org/10.1016/j.pocean.2014.12.005>.
- 1026 Planas, D., Agustí, S., Duarte, C. M., Granata, T. C., and Merino, M. (1999). Nitrate uptake and
1027 diffusive nitrate supply in the Central Atlantic. *Limnology and Oceanography* 44, 116–126.
1028 doi:[10.4319/lo.1999.44.1.0116](https://doi.org/10.4319/lo.1999.44.1.0116).
- 1029 Polyakov, I. V., Pnyushkov, A. V., Alkire, M. B., Ashik, I. M., Baumann, T. M., Carmack, E. C., et
1030 al. (2017). Greater role for Atlantic inflows on sea-ice loss in the Eurasian Basin of the
1031 Arctic Ocean. *Science* 356, 285–291. doi:[10.1126/science.aai8204](https://doi.org/10.1126/science.aai8204).
- 1032 Polzin, K. L., Naveira Garabato, A. C., Huussen, T. N., Sloyan, B. M., and Waterman, S. (2014).
1033 Finescale parameterizations of turbulent dissipation. *J. Geophys. Res. Oceans* 119, 1383–
1034 1419. doi:[10.1002/2013jc008979](https://doi.org/10.1002/2013jc008979).
- 1035 Rainville, L., and Woodgate, R. A. (2009). Observations of internal wave generation in the
1036 seasonally ice-free Arctic. *Geophysical Research Letters* 36. doi:[10.1029/2009GL041291](https://doi.org/10.1029/2009GL041291).
- 1037 Randelhoff, A., Fer, I., and Sundfjord, A. (2017). Turbulent Upper-Ocean Mixing Affected by
1038 Meltwater Layers during Arctic Summer. *Journal of Physical Oceanography* 47, 835–853.
1039 doi:[10.1175/JPO-D-16-0200.1](https://doi.org/10.1175/JPO-D-16-0200.1).
- 1040 Randelhoff, A., Fer, I., Sundfjord, A., Tremblay, J.-E., and Reigstad, M. (2016). Vertical fluxes
1041 of nitrate in the seasonal nitracline of the Atlantic sector of the Arctic Ocean. *Journal of*
1042 *Geophysical Research-Oceans* 121, 5282–5295. doi:[10.1002/2016JC011779](https://doi.org/10.1002/2016JC011779).
- 1043 Randelhoff, A., and Guthrie, J. D. (2016). Regional Patterns in Current and Future Export
1044 Production in the Central Arctic Ocean Quantified from Nitrate Fluxes. *Geophysical Research*
1045 *Letters*. doi:[10.1002/2016gl070252](https://doi.org/10.1002/2016gl070252).
- 1046 Randelhoff, A., Reigstad, M., Chierici, M., Sundfjord, A., Ivanov, V., Cape, M., et al. (2018).
1047 Seasonality of the Physical and Biogeochemical Hydrography in the Inflow to the Arctic
1048 Ocean Through Fram Strait. *Frontiers in Marine Science* 5. doi:[10.3389/fmars.2018.00224](https://doi.org/10.3389/fmars.2018.00224).

1049 Randelhoff, A., and Sundfjord, A. (2018). Short commentary on marine productivity at
 1050 Arctic shelf breaks: Upwelling, advection and vertical mixing. *Ocean Science* 14, 293–300.
 1051 doi:[10.5194/os-14-293-2018](https://doi.org/10.5194/os-14-293-2018).

1052 Randelhoff, A., Sundfjord, A., and Reigstad, M. (2015). Seasonal variability and fluxes of
 1053 nitrate in the surface waters over the Arctic shelf slope. *Geophysical Research Letters* 42,
 1054 3442–3449. doi:[10.1002/2015gl063655](https://doi.org/10.1002/2015gl063655).

1055 Redfield, A. C., Ketchum, B. H., and Richards, F. A. (1963). “The influence of organisms on
 1056 the composition of sea-water,” in *The Sea*, ed. M. N. Hill (Academic Press), 26–77.

1057 Rees, A. P., Joint, I., Woodward, E. M. S., and Donald, K. M. (2001). Carbon, nitrogen and
 1058 phosphorus budgets within a mesoscale eddy: Comparison of mass balance with in vitro
 1059 determinations. *Deep Sea Research Part II: Topical Studies in Oceanography* 48, 859–872.
 1060 doi:[10.1016/S0967-0645\(00\)00101-6](https://doi.org/10.1016/S0967-0645(00)00101-6).

1061 Renaud, P. E., Sejr, M. K., Bluhm, B. A., Sirenko, B., and Ellingsen, I. H. (2015). The future of
 1062 Arctic benthos: Expansion, invasion, and biodiversity. *Progress in Oceanography* 139, 244–
 1063 257. doi:[10.1016/j.pocean.2015.07.007](https://doi.org/10.1016/j.pocean.2015.07.007).

1064 Rippeth, T. P., Lincoln, B. J., Lenn, Y.-D., Green, J. A. M., Sundfjord, A., and Bacon, S. (2015).
 1065 Tide-mediated warming of Arctic halocline by Atlantic heat fluxes over rough topography.
 1066 *Nature Geoscience* 8, 191–194. doi:[10.1038/ngeo2350](https://doi.org/10.1038/ngeo2350).

1067 Rippeth, T. P., Wiles, P., Palmer, M. R., Sharples, J., and Tweddle, J. (2009). The diapycnal
 1068 nutrient flux and shear-induced diapycnal mixing in the seasonally stratified western Irish
 1069 Sea. *Continental Shelf Research* 29, 1580–1587. doi:[10.1016/j.csr.2009.04.009](https://doi.org/10.1016/j.csr.2009.04.009).

1070 Risgaard-Petersen, N., Revsbech, N. P., and Rysgaard, S. (1995). Combined microdiffusion-
 1071 hypobromite oxidation method for determining nitrogen-15 isotope in ammonium. *Soil*
 1072 *Science Society of America Journal* 59, 1077–1080.

1073 Rysgaard, S., Vang, T., Stjernholm, M., Rasmussen, B., Windelin, A., and Kiilsholm, S. (2003).
 1074 Physical Conditions, Carbon Transport, and Climate Change Impacts in a Northeast
 1075 Greenland Fjord. *Arctic, Antarctic, and Alpine Research* 35, 301–312. doi:[10.1657/1523-0430\(2003\)035\[0301:PCCTAC\]2.0.CO;2](https://doi.org/10.1657/1523-0430(2003)035[0301:PCCTAC]2.0.CO;2).

1077 Sakamoto, C. M., Johnson, K. S., and Coletti, L. J. (2009). Improved algorithm for the
 1078 computation of nitrate concentrations in seawater using an in situ ultraviolet
 1079 spectrophotometer. *Limnology and Oceanography: Methods* 7, {132–143}.

1080 Sakshaug, E. (2004). “Primary and Secondary Production in the Arctic Seas,” in *The Organic*
 1081 *Carbon Cycle in the Arctic Ocean*, eds. R. Stein and R. W. Macdonald (Springer Berlin
 1082 Heidelberg), 57–81. doi:[10.1007/978-3-642-18912-8_3](https://doi.org/10.1007/978-3-642-18912-8_3).

1083 Schafstall, J., Dengler, M., Brandt, P., and Bange, H. (2010). Tidal-induced mixing and
 1084 diapycnal nutrient fluxes in the Mauritanian upwelling region. *Journal of Geophysical*
 1085 *Research* 115, C10014. doi:[10.1029/2009JC005940](https://doi.org/10.1029/2009JC005940).

1086 Scheifele, B., Waterman, S., Merckelbach, L., and Carpenter, J. R. (2018). Measuring the
 1087 Dissipation Rate of Turbulent Kinetic Energy in Strongly Stratified, Low-Energy
 1088 Environments: A Case Study From the Arctic Ocean. *Journal of Geophysical Research: Oceans*
 1089 123, 5459–5480. doi:[10.1029/2017JC013731](https://doi.org/10.1029/2017JC013731).

1090 Schnetger, B., and Lehnert, C. (2014). Determination of nitrate plus nitrite in small volume
 1091 marine water samples using vanadium (III) chloride as a reduction agent. *Marine Chemistry*
 1092 160, 91–98.

1093 Sharples, J., Moore, C. M., and Abraham, E. R. (2001). Internal tide dissipation, mixing, and
 1094 vertical nitrate flux at the shelf edge of NE New Zealand. *Journal of Geophysical Research:*
 1095 *Oceans* 106, 14069–14081. doi:[10.1029/2000JC000604](https://doi.org/10.1029/2000JC000604).

1096 Sharples, J., Tweddle, J. F., Green, J. A. M., Palmer, M. R., Kim, Y.-N., Hickman, A. E., et al.
 1097 (2007). Spring-neap modulation of internal tide mixing and vertical nitrate fluxes at a shelf
 1098 edge in summer. *Limnology and Oceanography* 52, 1735–1747.
 1099 doi:[10.4319/lo.2007.52.5.1735](https://doi.org/10.4319/lo.2007.52.5.1735).

1100 Shih, L. H., Koseff, J. R., Ivey, G. N., and Ferziger, J. H. (2005). Parameterization of turbulent
 1101 fluxes and scales using homogeneous sheared stably stratified turbulence simulations.
 1102 *Journal of Fluid Mechanics* 525, 193–214. doi:[10.1017/S0022112004002587](https://doi.org/10.1017/S0022112004002587).

1103 Shiozaki, T., Furuya, K., Kodama, T., and Takeda, S. (2009). Contribution of N₂ fixation to
 1104 new production in the western North Pacific Ocean along 155E. *Marine Ecology Progress*
 1105 *Series* 377, 19–32. doi:[10.3354/meps07837](https://doi.org/10.3354/meps07837).

1106 Shiozaki, T., Furuya, K., Kurotori, H., Kodama, T., Takeda, S., Endoh, T., et al. (2011).
 1107 Imbalance between vertical nitrate flux and nitrate assimilation on a continental shelf:
 1108 Implications of nitrification. *Journal of Geophysical Research: Oceans* 116.
 1109 doi:[10.1029/2010JC006934](https://doi.org/10.1029/2010JC006934).

1110 Sipler, R. E., Gong, D., Baer, S. E., Sanderson, M. P., Roberts, Q. N., Mulholland, M. R., et al.
 1111 (2017). Preliminary estimates of the contribution of Arctic nitrogen fixation to the global
 1112 nitrogen budget. *Limnology and Oceanography Letters* 2, 159–166. doi:[10.1002/lol2.10046](https://doi.org/10.1002/lol2.10046).

1113 Spall, M. A., Pickart, R. S., Brugler, E. T., Moore, G. W. K., Thomas, L., and Arrigo, K. R. (2014).
 1114 Role of shelfbreak upwelling in the formation of a massive under-ice bloom in the Chukchi
 1115 Sea. *Deep Sea Research Part II: Topical Studies in Oceanography* 105, 17–29.
 1116 doi:<http://dx.doi.org/10.1016/j.dsr2.2014.03.017>.

1117 Stevens, J.-L. R., Rudiger, P., and Bednar, J. A. (2015). HoloViews: Building Complex
 1118 Visualizations Easily for Reproducible Science. in *Proceedings of the 14th Python in Science*
 1119 *Conference*.

1120 Stroeve, J. C., Serreze, M. C., Holland, M. M., Kay, J. E., Malanik, J., and Barrett, A. P. (2012).
 1121 The Arctic's rapidly shrinking sea ice cover: A research synthesis. *Climatic Change* 110,
 1122 1005–1027. doi:[10.1007/s10584-011-0101-1](https://doi.org/10.1007/s10584-011-0101-1).

- 1123 Sundfjord, A., Fer, I., Kasajima, Y., and Svendsen, H. (2007). Observations of turbulent
1124 mixing and hydrography in the marginal ice zone of the Barents Sea. *Journal of Geophysical*
1125 *Research: Oceans* 112. doi:[10.1029/2006JC003524](https://doi.org/10.1029/2006JC003524).
- 1126 Sverdrup, H. (1953). On conditions for the vernal blooming of phytoplankton. *ICES Journal*
1127 *of Marine Science* 18, 287–295.
- 1128 Tamelander, T., Reigstad, M., Olli, K., Slagstad, D., and Wassmann, P. (2013). New
1129 Production Regulates Export Stoichiometry in the Ocean. *PLoS ONE* 8, e54027.
1130 doi:[10.1371/journal.pone.0054027](https://doi.org/10.1371/journal.pone.0054027).
- 1131 Tank, S. E., Manizza, M., Holmes, R. M., McClelland, J. W., and Peterson, B. J. (2012). The
1132 Processing and Impact of Dissolved Riverine Nitrogen in the Arctic Ocean. *Estuaries and*
1133 *Coasts* 35, 401–415. doi:[10.1007/s12237-011-9417-3](https://doi.org/10.1007/s12237-011-9417-3).
- 1134 Torres-Valdés, S., Tsubouchi, T., Bacon, S., Naveira-Garabato, A. C., Sanders, R., McLaughlin,
1135 F. A., et al. (2013). Export of nutrients from the Arctic Ocean. *J. Geophys. Res. Oceans* 118,
1136 1625–1644. doi:[10.1002/jgrc.20063](https://doi.org/10.1002/jgrc.20063).
- 1137 Tremblay, J.-E., Anderson, L. G., Matrai, P., Coupel, P., Belanger, S., Michel, C., et al. (2015).
1138 Global and regional drivers of nutrient supply, primary production and CO₂ drawdown in
1139 the changing Arctic Ocean. *Progress in Oceanography* 139, 171–196.
1140 doi:[10.1016/j.pocean.2015.08.009](https://doi.org/10.1016/j.pocean.2015.08.009).
- 1141 Tremblay, J.-E., Simpson, K. G., Martin, J., Miller, L., Gratton, Y., Barber, D., et al. (2008).
1142 Vertical stability and the annual dynamics of nutrients and chlorophyll fluorescence in the
1143 coastal, southeast Beaufort Sea. *Journal of Geophysical Research-Oceans* 113, C07S90.
1144 doi:[10.1029/2007JC004547](https://doi.org/10.1029/2007JC004547).
- 1145 Valiela, I. (2015). *Marine ecological processes*. 3rd ed. Springer-Verlag New York.
- 1146 Vancoppenolle, M., Bopp, L., Madec, G., Dunne, J., Ilyina, T., Halloran, P. R., et al. (2013).
1147 Future Arctic Ocean primary productivity from CMIP5 simulations: Uncertain outcome, but
1148 consistent mechanisms. *Global Biogeochemical Cycles* 27, 605–619. doi:[10.1002/gbc.20055](https://doi.org/10.1002/gbc.20055).
- 1149 Watanabe, E., Onodera, J., Harada, N., Honda, M. C., Kimoto, K., Kikuchi, T., et al. (2014).
1150 Enhanced role of eddies in the Arctic marine biological pump. *Nature Communications* 5.
1151 doi:[10.1038/ncomms4950](https://doi.org/10.1038/ncomms4950).
- 1152 Wiedmann, I. (2015). Potential drivers of the downward carbon and particle flux in Arctic
1153 marine ecosystems under contrasting hydrographical and ecological situations.
- 1154 Wiedmann, I., Tremblay, J.-É., Sundfjord, A., and Reigstad, M. (2017). Upward nitrate flux
1155 and downward particulate organic carbon flux under contrasting situations of stratification
1156 and turbulent mixing in an Arctic shelf sea. *Elem Sci Anth* 5.
- 1157 Wiles, P. J., Rippeth, T. P., Simpson, J. H., and Hendricks, P. J. (2006). A novel technique for
1158 measuring the rate of turbulent dissipation in the marine environment. *Geophysical*
1159 *Research Letters* 33. doi:[10.1029/2006GL027050](https://doi.org/10.1029/2006GL027050).

1160 Woodgate, R. A., Weingartner, T. J., and Lindsay, R. (2012). Observed increases in Bering
1161 Strait oceanic fluxes from the Pacific to the Arctic from 2001 to 2011 and their impacts on
1162 the Arctic Ocean water column. *Geophysical Research Letters* 39.
1163 doi:[10.1029/2012GL054092](https://doi.org/10.1029/2012GL054092).